Istraživanje preferencije vezanja proteina HB6, RDM1 i DMS3 na BPM1

Tokić, Mirta

University of Zagreb
Faculty of Science
Department of Biology

Mirta Tokić

Preferential protein-protein binding of HB6, RDM1 and DMS3 to BPM1

Graduation thesis

Zagreb, 2019

Sveučilište u Zagrebu
Prirodoslovno-matematički fakultet
Biološki odsjek

Mirta Tokić

Istraživanje preferencije vezanja proteina HB6, RDM1 i DMS3 na BPM1

Diplomski rad

Zagreb, 2019.

Ovaj se diplomski rad proveo na Zavodu za molekularnu biologiju Prirodoslovno-matematičkog fakulteta Sveučilišta u Zagrebu, pod vodstvom izv. prof. dr. sc. Nataše Bauer. Rad se predao na ocjenu Biološkom odsjeku Prirodoslovno-matematičkog fakulteta Sveučilišta u Zagrebu radi stjecanja zvanja magistra molekularne biologije.

ACKNOWLEDGEMENTS

I sincerely express my gratitude to all the staff members of the Plant Molecular Biology Laboratory for their unfailing support and assistance in the past year. To Ana-Marija Boljkovac who has facilitated and quickened my adaptation to a new work environment. To Mateja Jagić who has always been eager to help in times of need. To Professor Dunja Leljak-Levanić who kindly invited me to this laboratory two years ago and has watched me progress through my experiment. To my mentor Professor Nataša Bauer who would always find a solution to any apparently unsolvable issue and encouraged me to continue pursuing science. To Lucija Markulin for her patience and support over the months. Last but by no mean least, a very special thanks to Andreja Škiljaica who has monitored my work from the beginning to the end and extended her helping hand whenever I needed it. Finally, I thank my parents and friends who have stood by my side for as long I can remember and have supported me throughout my education and beyond.

TEMELJNA DOKUMENTACIJSKA KARTICA

Sveučilište u Zagrebu
Prirodoslovno-matematički fakultet
Biološki odsjek Diplomski rad

Istraživanje preferencije vezanja proteina HB6, RDM1 i DMS3 na BPM1

Mirta Tokić

Rooseveltov trg 6, 10 000 Zagreb, Hrvatska

Sažetak

BPM proteini vrste *A. thaliana* usmjeravaju nekoliko transkripcijskih faktora u 26S proteasomsku razgradnju ovisnu o ubikvitinu. U preliminarnom istraživanju, nakon kopurifikacije proteina TAP-tag metodom iz klijanaca uročnjaka, pokazana je interakcija između proteina BPM1 i DMS3, odnosno RDM1, članova puta DNA metilacije usmjerene RNA molekulom (RdDM). U ovom diplomskom radu, interakcije između BPM1, transkripcijskog faktora HB6 te DMS3, odnosno RDM1 proteina, analizirane su metodom kopurifikacije (*pull-down*), jedan na jedan i jedan na dva. U tu su svrhu prikladni ekspresijski plazmidi konstruirani pomoću ligacije ili In-Fusion metode. Plazmidi su kemijski transformirani u *E. coli* soj Rosetta™. Nakon indukcije ekspresije gena, fuzijski su proteini pročišćeni afinitetnom kromatografijom i vizualizirani SDS-PAGE metodom, bojanjem proteina u gelu i imunodetekcijom. U ovom diplomskom radu, potvrđena je interakcija između RDM1 i BPM1, te DMS3 i BPM1. Interakcija između HB6 i BPM1-GST nije potvrđena, budući da se protein HB6 vezao i na GST (negativna kontrola). Ovi eksperimenti predstavljaju osnovu za daljnja istraživanja koja bi mogla razriješiti potencijalnu ulogu proteina BPM1 u putu RdDM.

(68 stranica, 20 slika, 4 tablice, 68 literaturnih navoda, jezik izvornika: engleski)

Rad je pohranjen u Središnjoj biološkoj knjižnici.

Ključne riječi: interakcija proteina, kopurifikacija, RdDM, degradacija proteina, BPM1, *Arabidopsis thaliana*

Voditelj: izv. prof. dr. sc. Nataša Bauer

Neposredni voditelj: dr. sc. Lucija Markulin

Ocjenitelji: izv. prof. dr. sc. Nataša Bauer
izv. prof. dr. sc. Željka Vidaković-Cifrek
izv. prof. dr. sc. Martina Šeruga Musić
Zamjena: izv. prof. dr. sc. Dunja Leljak-Levanić

Rad prihvaćen: 31. siječnja 2019.

BASIC DOCUMENTATION CARD

University of Zagreb
Faculty of Science
Department of Biology

Graduation thesis

Preferential protein-protein binding of HB6, RDM1 and DMS3 to BPM1

Mirta Tokić

Rooseveltov trg 6, 10 000 Zagreb, Croatia

Abstract

BPM proteins in *A. thaliana* are known to direct several transcription factors to ubiquitin-mediated 26S proteasome degradation. Preliminary investigation, after protein copurification by TAP-tag from *Arabidopsis* seedlings, has shown that BPM1 also potentially interacts with members of the RNA-directed DNA methylation (RdDM) pathway, DMS3 and RDM1. Here, interactions of BPM1 with transcription factor HB6 and proteins DMS3 and RDM1 were analyzed in one to one and one to two pull-down assays. For this purpose, suitable expression plasmids were generated using ligation or In-Fusion cloning methods. Rosetta^{TM} *E. coli* strain was chemically transformed with generated constructs. Protein expression was induced, and fusion proteins were purified. Finally, pull-down assays were performed and proteins visualized by SDS-PAGE, staining and immunodetection. In the conditions carried out here, RDM1 and DMS3 interacted with BPM1. Since HB6 interacted with both BPM1-GST and GST alone (negative control), a direct HB6 interaction could not be shown. These experiments provide a basis for future analyses which could elucidate the potential function of BPM1 in the RdDM pathway.

(68 pages, 20 figures, 4 tables, 68 references, original in: English)

Thesis deposited in the Central Biological Library.

Key words: protein interaction, pull-down, RdDM, protein degradation, BPM1, *Arabidopsis thaliana*

Supervisor: Dr. sc. Nataša Bauer, Assoc. Prof.

Assistant Supervisor: Dr. sc. Lucija Markulin

Reviewers: Dr. Sc. Nataša Bauer, Assoc. Prof.
Dr. Sc. Željka Vidaković-Cifrek, Assoc. Prof.
Dr. Sc. Martina Šeruga Musić, Assoc. Prof.

Replacement reviewer: Dr. Sc. Dunja Leljak-Levanić, Assoc. Prof.

Thesis accepted: January 31st 2019

Table of Contents

List of Abbreviations

Amp – Ampicillin
BPM – BTB/POZ (BTB) and MATH domain-containing protein
BTB – Bric à brac, Tramtrack and Broad complex/Pox virus and Zinc finger domain
CBB – Coomassie Brilliant Blue
cDNA – Complementary DNA
CDS – Coding region
Chl – Chloramphenicol
$CRL3^{BPM}$ – Cullin3-RING [Really interesting new gene] BPM E3 ligase
CUL3 – Cullin 3
DDR – DMS3, DRD1 and RDM1
DMS3 – Defective in meristem silencing 3
DNA – Deoxyribonucleic acid
DREB2A – Dehydration-responsive element-binding protein 2A
Fw primer – Forward primer
GSH – Glutathione
GST – Glutathione S-transferase
HB6 – Homeobox protein 6
His – Histidine
Kan – Kanamycin
MATH – Meprin and TRAF [Tumor necrosis factor receptor-associated factor] homology domain
MCS – Multiple cloning site
mRNA – Messenger RNA
Ni-NTA – Nickel-nitrilotriacetic acid
PCR –Polymerase chain reaction
Pol II/IV/V – RNA polymerase II/IV/V
PTGS – Posttranscriptional gene silencing
RdDM – RNA-directed DNA methylation
RDM1 – RNA-directed DNA methylation 1
RE – Restriction enzyme
Rev primer – Reverse primer
RNA – Ribonucleic acid
RNAi – RNA interference
RT – Room temperature
SDS-PAGE – Sodium dodecyl sulfate polyacrylamide gel electrophoresis
siRNA – Small interfering RNA
SmR – Streptomycin and spectinomycin
ssDNA – Single stranded DNA
TF – Transcription factor
TGS – Transcriptional gene silencing
tRNA – Transfer RNA
WRI1 – Wrinkled 1
β-met – β-mercaptoethanol

1 INTRODUCTION

Plants have had to, due to their sessile lifestyle, not only develop effective strategies to control mechanisms that regulate the timing of development and physiological processes but also to overcome environmental stress conditions such as drought or extreme temperatures. Regulating gene expression is the basis of all changes and responses in the cell. The mechanisms that enable all living organisms to grow, mature, reproduce and survive are transcriptional regulation that is governed by available transcription factors and by epigenetic modifications; posttranscriptional regulation that is dependent on mRNA processing, localization and degradation; translational and posttranslational regulation directed by protein synthesis, modification and turnover (Alberts et al., 2008).

1.1 RNA-DIRECTED DNA METHYLATION (RdDM)

The prefix *epi-* in epigenetics originates from the Greek word for "over", and appropriately, epigenetics represents a form of inheritance that is superior to the genetic inheritance based on DNA information. Studies through years have shed light into six different epigenetic mechanisms in eukaryotes: histone variants and histone covalent modifications, non-coding RNAs, architecture of the nucleus, chromatin remodeling and, the most studied epigenetic mark, DNA methylation. DNA methylation has been shown to have a diverse set of functions like regulating gene expression (activation or repression, depending on the sequence methylated), suppressing homologous recombination in repetitive sequences, defense against foreign DNA or chromatin condensation and stabilization. It is also a means by which the newly synthesized strand of DNA is distinguished from the template after DNA replication in eukaryotes and prokaryotes (Alberts et al., 2008). Plants have well-developed epigenetic regulation systems, some of which are plant-specific, indicating its essential role in plant physiology. RNA-directed DNA methylation (RdDM) pathway is one such example. The main function of the RdDM pathway is *de novo* methylation of DNA (methylation of a previously unmodified DNA sequence). That way RdDM plays a role in transposon control, pathogen defense, stress response, interallelic and intercellular communication. It also contributes to genomic imprinting, reproduction, and creation of epialleles (Haag and Pikaard, 2011; Zemach et al., 2013; Matzke and Mosher, 2014).

RNA interference (RNAi) is a further example of epigenetic mechanisms in eukaryotic cells.

They can act in a posttranscriptional gene silencing (PTGS) manner in the cytoplasm, sending target mRNA for degradation and repressing translation. In the nucleus, however, they can elicit transcriptional gene silencing (TGS) by directing repressive epigenetic modifications, such as DNA cytosine and histone methylation, to homologous regions of the genome (Matzke and Mosher, 2014).

RdDM pathway in plants is unique among other small RNA-mediated chromatin modifications because it depends on specialized transcriptional machinery that is centered around two plant-specific RNA polymerases called polymerase IV (Pol IV) and polymerase V (Pol V), which evolved through gene duplication of Pol II (Ream et al., 2009). Neither Pol IV nor Pol V are essential for plant viability. It is still unknown why plants posses two additional RNA polymerases and such a unique DNA methylation pathway (Ream et al., 2009; Haag and Pikaard, 2011). According to a proposed model (**Figure 1**), the Pol IV transcripts of DNA repeats are made double-stranded by RNA-dependent RNA polymerase 2 (RDR2) and are diced by Dicer-like 3 enzyme (DCL3) into 24-nt siRNAs which are then transported into cytoplasm where they bind (in single stranded form) to Argonaut 4 (AGO4) to form AGO4-RISC (RNA-induced silencing complex) complex. The complex returns into the nucleus and binds to transcripts of Pol V in a sequence dependent manner. Pol V is enriched at gene promoter regions and evolutionary young transposons. Genome-wide Pol V localization and transcription is dependent on DDR (which is named after its components: Defective in meristem silencing 3 (DMS3), Defective in RNA-directed DNA methylation 1 (DRD1) and RNA-directed DNA methylation 1 (RDM1) protein) complex. AGO4 interacts with both Pol V and RDM1 resulting in subsequent recruitment of Domains rearranged methyltransferase 2 (DRM2) which mediates *de novo* DNA methylation in CG, CNG or CNN DNA sites (where N represents A, T or C) (Wierzbicki et al., 2012; Matzke and Mosher, 2014).

RdDM pathway targets transposon and other repetitive wide range genomic regions, preferentially in euchromatic regions (intergenic transposons or repetitive sequences in their promoters, introns or even coding regions) based on signatures that are not yet fully understood (Wierzbicki et al., 2012; Matzke and Mosher, 2014). The recognition of pre-existing H3K9me marks by a subunit of Pol IV enzyme is assumed (Zhang et al., 2013). RdDM was also shown to be excluded to some extent from pericentromeric heterochromatin where epigenetic modification and heterochromatization mostly occur in a siRNA-independent manner (Zemach et al., 2013). Also, it is worth noting that besides the described canonical RdDM pathway, there seem to be other variants of this pathway with slightly different components and mechanisms involved (Matzke and Mosher, 2014). Up to this day at least 40 members of RdDM pathway have been identified and described, DMS3 and RDM1 being among them.

1.1.1 DMS3

Defective in meristem silencing 3 (DMS3) is an unusual structural maintenance of chromosomes (SMC) solo hinge domain containing protein that lacks the ATP-ase activity of authentic SMC proteins (Kanno et al., 2008) but that might be compensated with the activity of a similar protein DMS11 (Lorković et al., 2012). It was found that DMS3 is part of a putative chromatin-remodeling complex, called the DDR complex, of the RdDM pathway (Law et al., 2010). Besides DMS3, the DDR complex is comprised of DRD1 protein, a SWI2/SNF2-like remodeling factor and RDM1 (described below). In addition, the above mentioned DMS11 may be a part of this complex too (Lorković et al., 2012). DDR complex stabilizes Pol V association with chromatin and regulates Pol V transcriptional activity (Law et al., 2010) but the exact role of DMS3 in the DDR complex is still unknown.

1.1.2 RDM1

RNA-directed DNA methylation 1 (RDM1) is a small, plant-specific protein most likely having multiple roles in the RdDM pathway. As already mentioned, it is a part of DDR complex that assists Pol V transcription at target loci. During Pol V-mediated transcription, the AGO4-RISC complex is believed to bind the nascent Pol V transcript based on complementarity and recruits DRM2 to catalyze methylation at the homologous sites across the genome (Wierzbicki et al., 2012; Matzke and Mosher, 2014). RDM1 might play a critical role in this step as it is the only protein known to interact with both AGO4, DRM2 and additionally, single stranded methylated DNA (ssDNA) (**Figure 1;** Gao et al., 2010; Matzke and Mosher, 2014). Moreover, the localization of AGO4 in the nucleus has shown to be RDM1-dependent (Gao et al., 2010). As an ssDNA binding protein, RDM1 is most likely found at DNA replication or transcription sites. The notion of RDM1 at sites of transcription is consistent with the involvement and cooperation of DNA-dependent RNA polymerases Pol II, IV and V in RdDM (Zheng et al., 2009). It has been demonstrated that Pol V and RDM1 colocalize in the perinucleolar processing center but not in the nucleoplasm, where the majority of RdDM target loci presumably reside (Gao et al., 2010). RDM1 might therefore bind to single-stranded DNA at the sites of Pol V transcription in the perinucleolar processing center and at the sites of Pol II transcription in the nucleoplasm. This is supported by the interaction and colocalization between RDM1 and Pol II (Gao et al., 2010). It seems that there is a specialization of function between the scaffold transcript-producing Pol II and Pol V at different steps and/or different target loci of RdDM (Gao et al., 2010). Overall, RDM1 may have a role in linking siRNA production with pre-existing or *de novo* cytosine methylation in DNA, interacting with both Pol II in nucleoplasm and Pol V in perinucleolar processing center (Gao et al., 2010; Law et al., 2010).

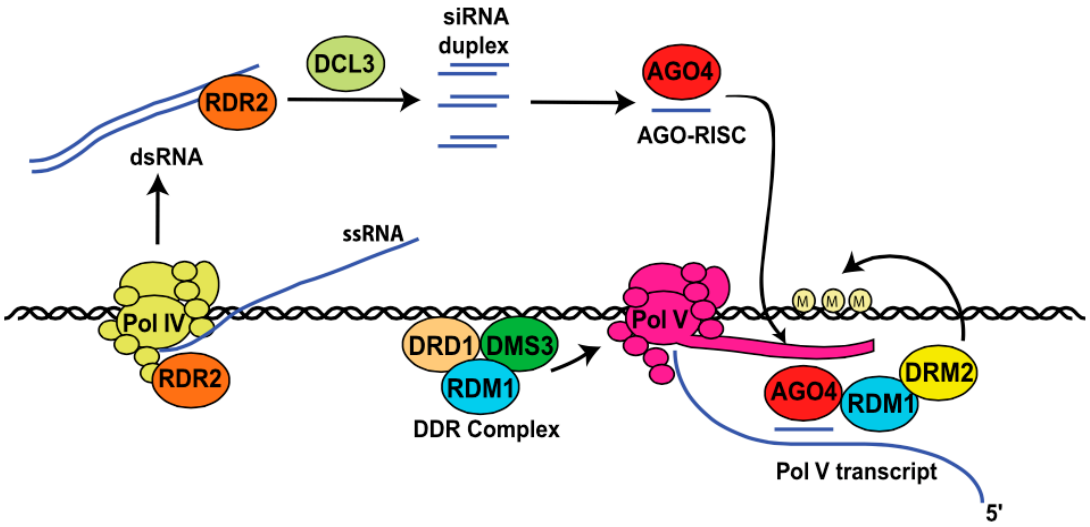

Figure 1. Simplified model for RNA-directed DNA methylation in *Arabidopsis thaliana*. RNA Pol IV transcripts are templates of RNA-dependent RNA polymerase 2 (RDR2). Resulting double stranded RNA is then cleaved by Dicer-like 3 (DCL3) into 24-nt siRNA products. One strand of 24-nt siRNA is loaded onto an Argonaute 4 (AGO4) RISC complex. Pol V localization and transcription is dependent on DDR complex and its nascent transcripts serve as scaffolds for the binding of AGO4–RISC complexes. In addition, AGO4 interacts with the Pol V and RDM1, and this complex localizes *de novo* DNA methyltransferase DRM2 and facilitate DNA methylation. (Image acquired from Wierzbicki et al., 2012).

1.2 PROTEIN DEGRADATION

Transcriptional and translational regulation enables proteome changes (synthesis of required proteins) in response to external and internal changes and signals. Proteins called transcription factors (TF) are responsible for controlling the transcription rate of target genes by binding to a specific sequence of DNA (Alberts et al., 2008). It should be noted that there are two types of transcription factors: general TF, which are essential for transcription to occur, and specific TF which can be further subdivided in two groups: transcription repressors and activators. In this way they contribute to, for example, stress tolerance, growth or reproduction. In most cases, however, stress tolerance is compromised to the detriment of plant growth and propagation, so it is necessary for plants to find a balance between survival and growth. Hence, transcription factors important for stress response must be rapidly removed after stress adaptation to enable normal growth (Yamaguchi-Shinozaki and Shinozaki, 2006).

1.2.1 Ubiquitin-mediated proteasomal protein degradation

Ubiquitin-dependent protein degradation is one of the most important posttranslational regulation of gene expression in eukaryotic cells. Ubiquitin is a small protein (8.5 kDa) which is added to lysine residues of target proteins in a cascade of reactions featuring three different enzymes in the three-step Ubiquitin-conjugating system (**Figure 2**). Ubiquitin-activating enzyme (E1), first in the series of enzymes, creates an activated, E1-bound ubiquitin that is subsequently transferred to one of a set of ubiquitin-conjugating (E2) enzymes which act in conjunction with E3 ubiquitin ligases. Together they form a complex where E3 binds specific substrates, helping E2 to ubiquitylate lysine residues of the substrate protein (Mazzucotelli et al., 2006; Alberts et al., 2008). A ubiquitin, having lysine residues itself, can be further conjugated by another ubiquitin moiety to form a polyubiquitin chain. The efficient polyubiquitylation is facilitated by multiubiquitin chain assembly E4 factors (Koegl et al., 1999). The most evident function of ubiquitylation is the targeting of proteins substrates to 26S proteasome degradation, but besides the elimination of aberrant or truncated proteins for cellular housekeeping, ubiquitylation regulates the amount of active proteins, which depend on the synthesis and degradation ratio (Mazzucotelli et al., 2006). It is yet not clear how ubiquitin can regulate the activity of target proteins. It could, however, serve as a ligand or maybe even change the conformation of target proteins (Mazzucotelli et al., 2006). Aside from its involvement in protein turnover, ubiquitylation seems to have other functions as well, seemingly dependent on the number of ubiquitin units in the chain linked to the target protein and on the lysine residue of ubiquitin utilized for the formation of polyubiquitin chain (Mazzucotelli et al., 2006; Gingerich et al., 2007).

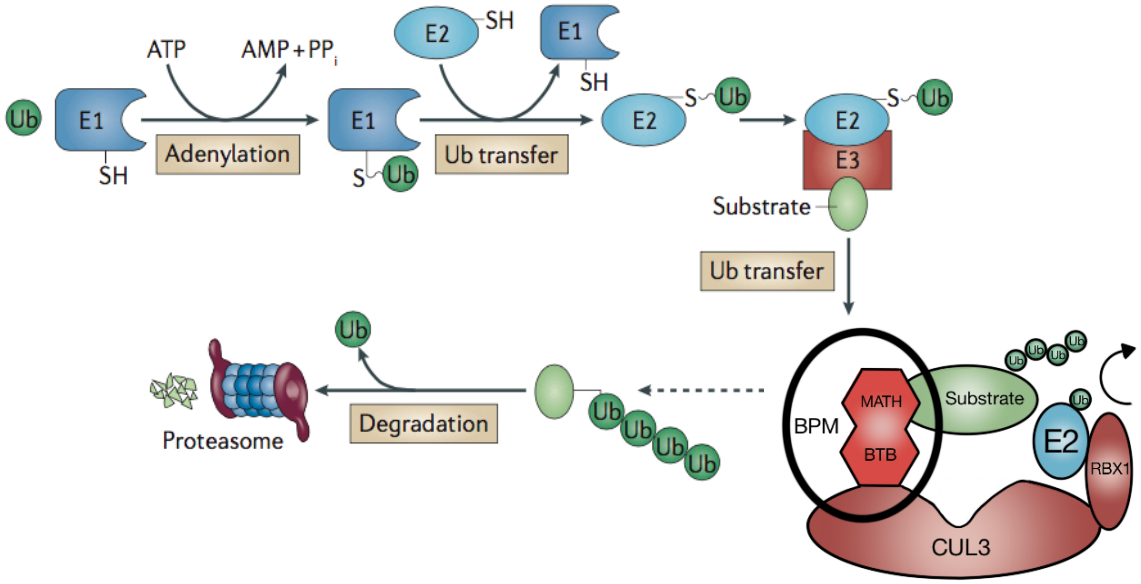

Figure 2. Protein degradation via 26S proteasome after ubiquitylation. It consists of a cascade of E1 ubiquitin-activating, E2 ubiquitin-conjugating and E3 ubiquitin ligase enzymes. E1 adenylates the C-terminal carboxylate of ubiquitin (Ub) forming a Ub thioester intermediate (E1-Ub). The ubiquitin is then transferred to E2 from which, with assistance of E3, is transferred to target protein. The CUL3-BPM ligase complex consists of a CUL3 protein, RING box 1 (RBX1) protein that associates with the E2 enzyme and a BTB/POZ-MATH (BPM) protein (circled) which is bound to CUL3 per BTB domain and target protein via MATH domain. (Adaped from van den Heuvel, 2004 and Maupin-Furlow, 2011).

1.2.2 CUL3 E3 ligases

E3 ubiquitin ligases are very well studied in model organisms such as *Arabidopsis thaliana*. The huge size of its E3 ubiquitin ligase gene family suggests a very complex role of these proteins as they are shown to participate in plant development and hormone signaling regulation (Mazzucotelli et al., 2006). E3 ligases can be classified into two groups depending on the presence of a HECT (Homology to E6-AP C-terminus) or a RING (Really interesting new gene)/U box domain. RING proteins can act as a single protein or as a component of complexes. Such multisubunit E3 ligases consist of two functional modules. One is the catalytic module included in a subunit of the RING protein (RING box protein 1, RBX1) that binds E2 (**Figure 2**). The second module specifically recognizes target substrates for ubiquitylation and is called accordingly, adapter. The same catalytic module

can bind many different adapters, therefore many different E3 complexes can be formed, which in turn catalyze the ubiquitylation of different substrates. The two modules are brought together by a Cullin (or Cullin-like) protein which acts as a molecular scaffold (**Figure 2;** Mazzucotelli et al., 2006). A well known Cullin protein is the Cullin 3 (CUL3) hence the name CUL3 E3 ligase. One possible adapter is BTB/POZ (Bric a brac, Tramtrack and Broad complex/Pox virus and Zinc finger) domain-containing protein (Gingerich et al., 2005; Weber et al., 2005).

1.2.3 BTB-MATH domain-containing proteins

The BTB-MATH protein family contains a BTB/POZ (BTB) domain located at the C-terminus and a Meprin and TRAF Homology (MATH) domain located close to N-terminus (Weber et al., 2005). The BTB domain contains around 116 amino acids that form a structure consisting of six α-helices and five β-sheets (Ahmad et al., 1998) which facilitate homo- and heterodimerization (Weber et al., 2005). The MATH domain comprises around 150 amino acids forming eight β-sheets (Sunnerhagen et al., 2002). As the name suggests, the motif was noted on the basis of homology with the C-terminal region of meprins A and B and the TRAF-C domain which also facilitates protein-protein interaction. Proteins consisting of both BTB and MATH domains are common in plants. *A. thaliana* has six genes for BTB-MATH containing proteins, referred to as the BPM1-6 which interact with CUL3 or other BTB containing proteins via eponymous domain (Weber et al., 2005) while substrate recognition is mediated by the MATH domain (Pintard et al., 2003). These proteins therefore act as substrate-binding adapters for the Cullin 3-based E3 ubiquitin ligase (**Figure 2**). Lechner et al. (2011) showed that *BPM* genes are expressed in all organs that were tested with similar tissue or organ-specific expression patterns. *BPMs* seem to have an elevated expression rate in floral buds and open flowers but significantly lower rates in siliques. *BPM1-3* were also found to have a strong expression in the pollen (Lechner et al., 2011). BPMs were shown to be functionally redundant but only some (e.g. BPM1) exhibit elevated expression in drought stress conditions (Weber and Hellmann, 2009). The BPM1-6 proteins were localized in the nucleus as well as the cytoplasm, leading researchers to believe that proteins can be ubiquitylated via CUL3 and potentially marked for degradation

in both cytoplasm and nucleus (Weber and Hellmann, 2009; Lechner et al., 2011). As suggested in Leljak-Levanić et al. (2012), BPMs may also have different functions, depending on their localization. BPMs could mediate protein degradation in the cytoplasm and regulate degradation-independent processes in the nucleus (more accurately, perinucleolar regions). This has been supported by BPM1 signal detection in the nucleolus (a nuclear department where TGS and RNA processing take place), which interestingly, did not colocalize with CUL3 signals (Leljak-Levanić et al., 2012). Because RdDM components were observed in the perinucleolar space (Gao et al., 2010) and preliminary experiments showed DMS3 and RDM1 as BPM1 interacting partners (Bauer et al., 2014), a CUL3 independent function in RdDM pathway for BPM1 was proposed. This was also supported by the preliminary finding that overexpression of BPM1 globally influenced DNA methylation.

BPM1 interacts with various TF: Dehydration-responsive element-binding protein 2A (DREB2A) (Morimoto et al., 2017), Homeobox protein 6 (HB6) (Lechner et al., 2011), Wrinkled 1 (WRI1) (Weber and Hellmann, 2009) and MYB domain protein 56 (MYB56) (Chen et al., 2015). All of these transcription factors have been shown to be destabilized as a consequence of this interaction.

1.2.4 DREB2A

Dehydration-responsive element-binding protein 2A (DREB2A), an APETALA2/ethylene-responsive element binding protein-type (AP2/ERF) transcription factor also known as C-repeat binding factor (CBF), is a key factor regulating the transcription of genes involved in ABA-independent drought, salt and heat stress response (Sakuma et al., 2006; Morimoto et al., 2017). Its activity is mediated by binding to *cis*-acting dehydration-responsive element/C-repeats (DRE/CRT; Sakuma et al., 2006).

DREB2A was shown to be involved in three different degradation pathways mediated by different interaction partners. One is the degradation via interaction with two C3HC4 RING domain-containing protein E3 ligases, DREB2A-interacting proteins 1 and 2 (DRIP1/2) (Qin et al., 2008). The second is by binding Radical-induced cell death 1 (RCD1) to its C-terminal region (Vainonen et al., 2012). And lastly, the interaction between DREB2A and BPM-CUL3 E3 ligase ($CRL3^{BPM}$) (Morimoto et al., 2017) which is responsible for the destabilization of DREB2A via the negative regulatory domain (NRD). This domain contains a PEST sequence (a peptide sequence rich in proline [P], glutamic acid [E], serine [S], and threonine [T]) (Sakuma et al., 2006). DREB2A was shown to be expressed at low levels even in the absence of stress, and rapidly turned over by the 26S proteasome (Qin et al., 2008; Morimoto et al., 2017). Such a rapid turnover of DREB2A enables plants to quickly fine-tune DREB2A protein levels depending on the environmental conditions. When heat or drought stress arise, DREB2A is stabilized and acts as a TF but is then rapidly degraded via BPMs to prevent growth inhibition (Morimoto et al., 2017). The mechanism of DREB2A stabilization and subsequent degradation remains unclear as is the stress signal–dependent activation mechanism of DREB2A. It is possible that DREB2A is posttranslationally modified or that unidentified interactors modulate its stability and activity to escape the multiple associated degradation pathways during early stress response (Morimoto et al., 2017).

1.2.5 HB6

Homeobox protein 6 (HB6) is a member of the homeobox-leucine zipper (HD-ZIP) transcription factor family class I which consist roughly of a homeodomain (DNA binding domain) and a leucine zipper domain (protein binding domain) for homo- or heterodimerization (Harris et al., 2011). HB6 is a transcription factor that negatively regulates abscisic acid (ABA) signaling pathway. ABA is a phytohormone that acts upon negative environmental cues like high osmolarity and low temperature and thereby stimulates physiological adaptations like stomatal closure, growth inhibition and differential gene regulation for metabolic and developmental adjustment. ABA stimulates and stabilizes HB6 (Lechner et al., 2011) which then reduces sensitivity of plant tissues for ABA during seed germination and stomatal closure (Himmelbach et al., 2002). As a TF it can not only (co)activate transcription of target genes by binding to defined *cis*-regulatory elements (pseudopalindromic core motif, CAATTATTA), but also its own (Himmelbach et al., 2002). HB6 functions as a transcription repressor as well, by negatively regulating the expression of some proteins (Lechner et al, 2011).

Interaction between HB6 and BPMs was demonstrated by yeast two hybrid (Y2H) and pull-down assay (Lechner et al., 2011). BPM1 interacts with the leucine zipper domain of HB6 but not with its homeodomain, thus potentially interfering with homo- or heterodimerization with other HD-Zip proteins but not (directly) with homeodomain-mediated DNA-binding (Lechner et al., 2011). Based on their overall result, the researchers proposed that $CRL3^{BPM}$ E3s trigger HB6 destruction in the absence of stress, when growth conditions are favorable, but upon stress, HB6 protein accumulates as a consequence of increased transcript accumulation and protein stability to trigger the expression and repression of downstream genes, of which at least some are involved in ABA desensitization. How this stabilization occurs is still unknown (Lechner et al., 2011).

1.2.6 WRI1

Wrinkled 1 (*WRI1*) gene encodes a member of the APETALA 2 (AP2) /ethylene-responsive element binding protein (EREBP) subfamily of transcription factors which are involved in embryo development, in particular the late maturation phase in which triacylglycerols accumulate in the seed. More precisely, it is involved in fatty acid synthesis and glycolysis (Focks and Benning, 1998; Maeo et al., 2009). Some mutations in *WRI1* cause a severe carbon flux reduction from sugars to pyruvate in the plastidial glycolytic pathway (Focks and Benning, 1998) consequently causing shrunken seeds with wrinkled shape, from which the name of the gene originated. WRI1 was shown to bind a so called AW box (Maeo et al., 2009). AW box is a proximal upstream region of genes that participate in the uptake of glycolytic intermediates into plastids, conversion to acetyl-CoA and malonyl-CoA, and the synthesis of fatty acids from them. By binding to them, WRI11 activates their transcription (Maeo et al., 2009; Grimberg et al., 2015). Conversely, WRI1 was also found to bind to genes related to photosynthesis and starch degradation promoting their down-regulation (Grimberg et al., 2015).

WRI1 was shown to interact with BPM proteins in yeast two hybrid assay and also shown to form complexes with BPMs at DNA level (Chen et al., 2013). By binding WRI1, BPMs regulate not only the stability of this protein, but also its activity (Chen et al., 2013). Apart from that, other regulation mechanisms have been identified. One is a C-terminal IDR3 (Intrinsically disordered region 3) destabilizing PEST motif that is not a BPM binding site and whose removal or mutation stabilized WRI1 (Chen et al., 2013). Also, it was shown that phosphorylated residues T70 and S166 made WRI1 more prone to protein degradation in cell-free extracts (Zhai et al., 2017). Additionally, a 14-3-3 binding motif which appeared to overlap with that for BPM protein binding site, was discovered (Ma et al., 2016). That would mean that binding members of the 14-3-3 phosphopeptide-binding protein group would interfere with BPM1 binding to WRI1, thereby protecting it from degradation. Moreover, the mentioned phosphorylated residues are very close to 14-3-3 binding site, suggesting signal interference (Zhai et al., 2017).

1.2.7 MYB56

MYB domain protein 56 (MYB56) is a member of R2R3-MYB transcription factor superfamily, the third family of transcrition factors found to interact with BPMs (Chen et al., 2015). MYB56 was shown to interact with all six membrs of BPM family (BPM1-6) in Y2H assay which caused its instability and degradation (Chen et al., 2015). In the same paper, $CRL3^{BPM}$ E3 ligases and MYB56 are proved to assemble at DNA level. MYB56 is described as a negative regulator of flowering by controlling expression of the *Flowering locus T* (*FT*). By $CRL3^{BPM}$–mediated MYB56 degradation, BPMs seem to have a positive effect on flowering (Chen et al., 2015).

1.3 THESIS OBJECTIVE AND AIMS

BPM1 was shown to interact with transcription factors DREB2A (Morimoto et al., 2017), HB6 (Lechner et al., 2011) and WRI1 (Weber and Hellmann, 2009) in a ubiquitin-mediated degradation manner. Based on a recent study, a potential CUL3-independent function of BPM1 protein has been proposed (Leljak-Levanić et al., 2012). Preliminary research has demonstrated that BPM1 interacts with both RDM1 and DMS3 in *in tandem* affinity purification of BPM1-TAP from cell extract of *A. thaliana* (Bauer et al., 2014) and later in yeast two hybrid assay.

The first aim of this thesis was to construct recombinant plasmid vectors suitable for protein expression in *Escherichia coli*. Five different genes (*DREB2A, DMS3, HB6, RDM1, WRI1*) were cloned.

A further objective was to overexpress seven fusion proteins BPM1-GST, DMS3-His, DMS3-GST, DREB2A-His, HB6-His, RDM1-His and WRI1-His in *E. coli* and to purify them with established optimized protocols.

In addition, the aim was to test *in vitro* interaction of BPM1 protein with different proteins by using pull-down assay, and to compare the binding affinity of BPM1 for HB6 and for RDM1 or DMS3.

2 MATERIALS AND METHODS

2.1 MATERIALS

2.1.1 Gene sequences

Full-length DNA coding sequences (CDS) of five *Arabidopsis thaliana* genes: *DMS3* (At3g49250), *DREB2A* (At5g05410.1), *HB6* (At2G22430.1), *RDM1* (At3g22680) and *WRI1* (At3g54320.1), were found in the National Center for Biotechnology Information (NCBI) and the Arabidopsis Information Resource (TAIR) databases. Their sequences were analysed in SnapGene Viewer (Version 4.1.6., GSL Biotech). Obtained gene inserts for *DMS3*, *DREB2A*, *HB6, RDM1* and *WRI1* (as described in sections 2.1.3 and 2.2.1) were used for cloning.

2.1.2 Primers

Primers for *DREB2A, DMS3* and *WRI1* amplification were designed with the online Clonetech In-Fusion Cloning Tool (https://www.takarabio.com/learning-centers/cloning /in-fusion-cloning-tools) and were ordered from Macrogen. Working solutions were prepared in ultrapure water (MiliQ®, TaKaRa) diluting a 100 pmol/µl stock solution to 10 pmol/µl. Both stock and working solutions were stored at -20 °C. Primer sequences are given in **Table 1**.

Table 1. List of primers used for In-Fusion cloning for *DREB2A, DMS3* and *WRI1*. The sequences point from 5' to 3' end. Underlined are sequences complementary to linearized target vector and red are restriction palindrome sequences recognized by specific restriction enzymes. The rest of the sequence is complementary to the gene.

Primer	Primer sequence (5'-3')	Product size
InF_DREB2A_Fw	ATGGGATCCGGAATTCTTATGGCAGTTTATGATCAGAGTGG	1040 bp
InF_DREB2A_Rev	GTAGGCCTTTGAATTCTTAGTTCTCCAGATCCAAGTAACTC	
InF_DMS3_Fw	GGTTCCGCGTGGATCCATGTATCCGACTGGTCAACA	1296 bp
InF_DMS3_Rev	GTCGACCCGGGAATTCTCATCTGGGTGTGTTCATTGG	
InF_WRI1_Fw	GGGCGCCATGGGATCCATGAAGAAGCGCTTAACCACTTCC	1349 bp
InF_WRI1_Rev	GTAGGCCTTTGAATTCTTATTCAGAACCAACGAACAAGCCC	

2.1.3 Plasmids

Sequences of all plasmids used here were found in the Addgene Vector Database (https://www.addgene.org/vector-database/). Gene constructs were virtually designed and analyzed (e.g. restriction and primer binding sites) in SnapGene Viewer (Version 4.1.6., GSL Biotech). Final constructs were sequenced in service (Macrogen Europe, The Netherlands) and analysed with Clustal × (Larkin et al., 2007). For protein expression, pET28a (+) (EMD Biosciences), pPROEx HTb (Invitrogen) and pGEX-4T-1 (Amersham) were used here. Provided were initial vectors used for gene amplification (pB7WGF-DMS3, pGAD424-HB6, pGAD424-RDM1, pCR8-WRI1), target vectors (pPROEx-KAT, pGEX4T1 and pET28a) and two additional plasmid constructs pET28a-DMS3 (Lorković et al., 2012) and pGEX4T1-BPM1 (**Figure 3**).

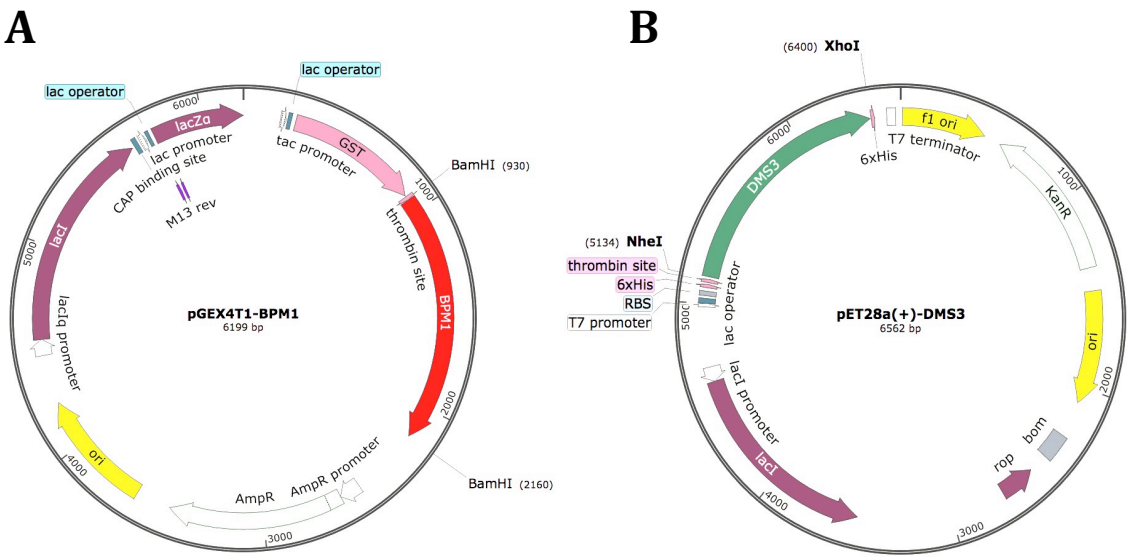

Figure 3. Plasmid maps of pGEX4T1-BPM1 **(A)** and pET28a-DMS3 (Lorković et al., 2012) **(B)** used for BPM1 and DMS3 protein expression respectively. Apart from a selection marker, an ori site for plasmid replication and a multiple cloning site (MCS), expression plasmids also contain sequences for a protein tag (GST or 6× His), a strong inducible promoter and a regulatory region upstream of the MCS, a transcription terminator and *lacI* gene which encodes a repressor protein.

2.1.4 Protein sequences

With online ExPASy Translate tool (https://web.expasy.org/translate), amino acid composition of fusion proteins was determined and with ProtParam tool (https://web.expasy.org/protparam/) theoretical values of molecular weight (Mw), number of amino acids (N) isoelectric point (pI), instability index (II) and aliphatic index (AI) were obtained (**Table 2**).

Table 2. Theoretical values of number of amino acids (N), molecular weight (Mw), isoelectric point (pI), instability index (II) and aliphatic index (AI) for different fusion proteins used in this study. The values were obtained from web tool ProtParam.

Fusion protein	N	Mw/kDa	pI	II	AI
BPM1-GST	633	71.02	6.54	33.41	89.00
DMS3-GST	646	73.06	6.46	39.26	85.14
DMS3-His	442	49.08	7.26	40.14	81.20
DREB2A-His	366	41.36	5.34	48.35	53.01
HB6-His	339	38.39	4.88	70.34	65.31
RDM1-His	198	22.38	5.91	60.76	68.94
WRI1-His	466	52.67	5.28	63.97	54.89

2.1.5 Bacterial strains and growth conditions

Escherichia coli competent cloning strains C2987H (NEB 5-alpha Competent *E. coli*, BioLabs) (https://www.neb.com/products/c2987-neb-5-alpha-competent-e-coli-high-efficiency# Product Information), XL10 Gold (Stratagene) and Stellar™ (HST08 Competent *E. coli*, Clontech) (https://www.takarabio.com/products/cloning/ competent-cells/stellar-chemically-competent-cells) were used for plasmid regeneration. Competent expression strain Rosetta™ (Novagen MSDS) (http://www.merckmillipore.com/INTL /en/product/RosettaDE3-Competent-Cells-Novagen,EMD_BIO-70954) was used for transformation with expression plasmids and recombinant protein expression. All strains were incubated on LB agar or liquid LB medium supplemented with appropriate antibiotics at 37 °C. Liquid cultures were agitated at 150-300 rpm.

2.1.6 Growth media

2.1.6.1 SOC medium

For competent cell recovery after heat shock in the transformation procedure SOC (Super Optimal Broth with Catabolic repression) medium (2% peptone or tryptone, 0.5% yeast extract, 10 mM NaCl, 2.5 mM KCl, 10 mM $MgCl_2$, 10 mM $MgSO_4$, 20 mM Glc) was used.

2.1.6.2 LB medium

LB (Lysogeny Broth) medium (1% tryptone, 0.5% yeast extract, 0.17 M NaCl) was used for bacterial growth. Bacterial plates were supplemented with agar for solidification. For selection, antibiotic ampicillin (c_{Amp} = 100 mg/ml), kanamycin (c_{Kan} = 50 mg/ml), spectinomycin (c_{SmR} = 50 mg/ml) or chloramphenicol (c_{Chl} = 34 mg/ml) were added to medium to a final concentration of 0.1 mg/ml for Amp, 0.05 mg/ml for Kan and SmR and 0.034 mg/ml for Chl.

2.1.7 Buffers

2.1.7.1 PBS buffer

For pull-down reaction and protein purification procedure, 1× PBS (Phosphate Buffered Saline) buffer (137 mM NaCl, 2.7 mM KCl, 10 mM Na_2HPO_4, 1.8 mM KH_2PO_4, pH 7.3) was used.

2.1.7.2 TAE buffer

For DNA gel electrophoresis, TAE (1× Tris Acetate EDTA) buffer (40 mM Tris-HCl pH 8.3, 1 mM EDTA) was used.

2.1.7.3 5× SB buffer

In SDS-PAGE, protein samples were mixed with sample loading buffer (5× SB) (125 mM Tris-HCl pH 6.8, 4% SDS, 32% glycerol, 10% β-mercaptoethanol, 0.01% bromophenol blue) before loading onto gel.

2.1.7.4 Bacteria lysis buffers

Lysis (extraction) buffer in the protein purification procedure differed between proteins. Bacteria expressing histidine (6× His)-tagged proteins were lysed in His lysis buffer that contained 50 mM Tris-HCl pH 8, 300 mM NaCl, 1 mM β-mercaptoethanol (β-met; Sigma Life Science), 10 mM imidazole (Sigma Aldrich) and 0.5% Triton X-100 supplemented with 1× Inhibitor cocktail (Complete Ultra Tablets Mini EDTA-free Easy pack, Roche). Bacteria expressing glutathione S-transferase (GST)-tagged proteins were lysed in GST lysis buffer 1 which contained 1× PBS and 0.1% Triton X-100 or in GST lysis buffer 2 containing 50 mM Tris-HCl pH 8, 150 mM NaCl, 10% glycerol, 0.5% NP-40 and 1 mM β-met supplemented with 1× Inhibitor cocktail.

2.1.7.5 Washing buffers

Washing buffer solutions, W1 (50 mM Tris-HCl pH 8, 20 mM imidazole, 1 mM β-met, 1 M NaCl), W2 (50 mM Tris-HCl pH 8, 20 mM imidazole, 1 mM β-met, 500 mM NaCl) and W3 (50 mM Tris-HCl pH 8, 20 mM imidazole, 1 mM β-met, 150 mM NaCl) were used for 6× His-tagged protein purification. GST-tagged proteins were washed with 1× PBS in some cases supplemeted with 0.05% Tween 20.

2.1.7.6 Elution buffer

Elution buffer (50 mM Tris-HCl pH 8, 150 mM NaCl, 500 mM imidazole) was used for 6× His-tagged protein elution.

2.1.7.7 Transfer buffer

Electroblotting in western blot was performed in transfer buffer (3.39 g/l Tris-HCl, 14.4 g/l Gly, 100 ml/l MetOH).

2.1.8 Commasie Brilliant Blue solution

For membrane staining after immunedetection, Coomassie stain, 50% MetOH, 7% acetic acid, 0.1% Coomassie Brilliant Blue R (CBB), was used. For destaining, membranes were incubated first in 50% methanol and 7% acetic acid, then in 90% methanol and 10% acetic acid, and finally washed with distilled water.

2.1.9 Molecular markers

In DNA agarose gel electrophoresis, Gene Ruler 1 kb (Thermo Scientific) was used for DNA analysis (**Figure 4A**).

For SDS-PAGE protein analysis, Page Ruler™ Plus Prestained Protein Ladder (Thermo Scientific) (**Figure 4B**) or Unstained Protein Molecular Weight Marker (Thermo Scientific™ Pierce™) (**Figure 4C**) were used.

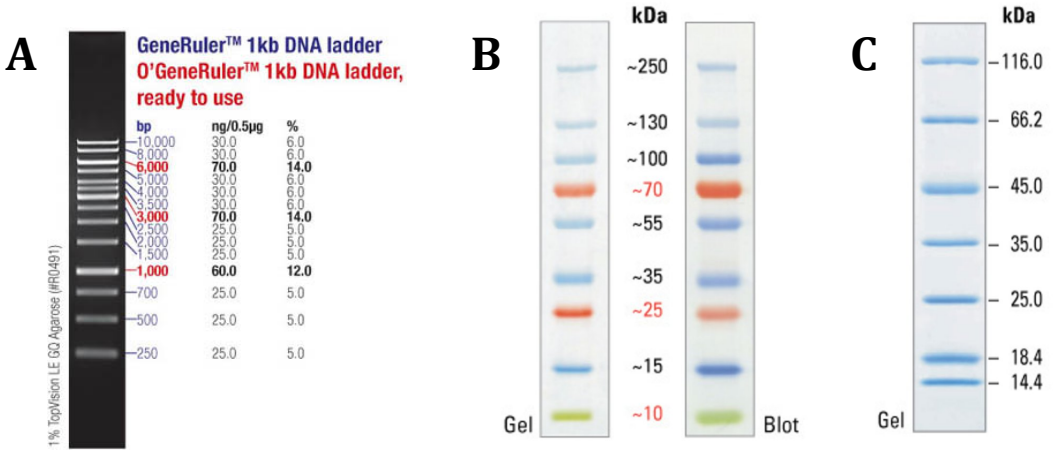

Figure 4. Gene Ruler 1 kb (Thermo Scientific) **(A)** was used to analyse DNA in agarose gel electrophoresis. Protein rulers Page Ruler™ Plus Prestained Protein Ladder (Thermo Scientific) **(B)** and Unstained Protein Molecular Weight Marker (Thermo Scientific™ Pierce™) **(C)** were used to analyze proteins in SDS-PAGE. (Images acquired from https://www.thermofisher.com/).

2.2 METHODS

Due to its short generation time, large seed production and relatively small genome size that has been completely sequenced, *Arabidopsis thaliana* was very early on used as a model organism for plants (Alberts et al., 2008) and a very large number of published works were based on analysis of this species. Gene sequences that are described and used in this thesis all stem from *A. thaliana*. Bacteria *Escherichia coli* was chosen as the host organism for the production of proteins encoded by the very same genes. It is easily grown in culture bottles and adapts to various conditions, reproduces rapidly and can easily be selected. Moreover, different strains were designed to enable plasmid amplification or protein overexpression from different species serving as a favorable heterologous system (Duong-Ly and Gabelli, 2014).

2.2.1 PLASMID CONSTRUCTION

Full-length coding regions of *DMS3*, *DREB2A*, *HB6*, *RDM1* and *WRI1* genes were obtained from either previously cloned plasmid vectors or a reverse transcribed mRNA extract from *Arabidopsis thaliana* (**Table 3**). Gene inserts were obtained by restriction digestion (for ligation-based cloning) or PCR (for In-Fusion cloning). Target vectors were linearized by restriction digestion. Insert and target vector were separated on gel, purified and cloning was performed by ligation or In-Fusion method. All procedures are explained in the following chapters.

Table 3. List of initial, target and final constructs used for cloning. Fusion tags of proteins (histidine, 6× His or glutathione S-transferase, GST) refer to the target vector that carries the defined N-terminal tag. In addition, restriction enzyme/s and methods used in gene cloning for each construct are given. Antibiotic resistance used for selection of transformed bacteria are written in brackets, where Amp stands for ampicillin, Kan for kanamycin and SmR streptomycin and spectinomycin.

Gene	Initial construct	Target vector	Fusion tag	Restriction enzyme/s	Final construct	Method
DMS3 **(At3g49250)**	pB7WGF-DMS3 (SmR)	pGEX4T1 (Amp)	GST	BamHI EcoRI	**pGEX4T1-DMS3 (Amp)**	In-Fusion
DREB2A **(At5g05410.1)**	cDNA DREB2A	pPROEx (Amp)	6× His	EcoRI	**pPROEx-DREB2A (Amp)**	In-Fusion
HB6 **(AT2G22430.1)**	pGAD424-HB6 (Amp)	pPROEx-KAT (Amp)	6× His	BamHI XbaI	**pPROEx-HB6 (Amp)**	Ligation
RDM1 **(At3g22680)**	pGAD424-RDM1 (Amp)	pET28a (Kan)	6× His	EcoRI HindIII	**pET28a-RDM1 (Kan)**	Ligation
WRI1 **(At3g54320.1)**	pCR8-WRI1 (SmR)	pPROEx-KAT (Amp)	6× His	EcoRI BamHI	**pPROEx-WRI1 (Amp)**	In-Fusion

2.2.1.1 Generation of PCR inserts for In-Fusion

PCR reaction was preformed using initial vectors as templates. The master mix was based on the manufacturer's instructions (CloneAmp^{TM} HiFi PCR Premix, Clontech). A DNA template (1 ng) as well as 7.5 pmol gene specific forward and reverse primer (**Table 1**) were added to a 25 µl reaction volume. The PCR program was set to 35 cycles of denaturation at 98 °C for 10 s, annealing at 55 °C for 10 s and extension at 72 °C for 5 s/kb (Gene Amp PCR System 2700, Applied Biosystems). PCR amplicons were visualized by 0.8% agarose gel electrophoresis and, after purification, concentration of PCR generated DNA fragments was measured.

2.2.1.2 Restriction digestion

To cut out coding sequences of desired genes from initial vectors, endonuclease restriction sites on both initial and target plasmid vectors were carefully analyzed and the best possible restriction endonucleases (RE) that enable insertion of desired gene in frame with tag were chosen (**Table 3**).

2.2.1.2.1 Preparatory restriction digestion

The reaction mixture was prepared so that the final reaction volume reached 40 µl according to the manufacturer's instructions (Fast Digestion of DNA, Thermo Scientific). A mass of 1 µg of DNA was inserted into reaction mixture with appropriate RE (Fast Digest, Thermo Scientific). The solutions were incubated for 1 h at 37 °C. DNA fragments were separated by 0.8% agarose gel electrophoresis. Wanted bands were excised from gel and concentration of purified DNA fragments was measured.

2.2.1.2.2 Control restriction digestion

After plasmid isolation, to verify presence of insert, restriction digestion was performed mainly with the same RE used for cloning. For verification purposes, 5 µl of DNA (20-100 ng/µl) was digested in total volume of 20 µl according to the manufacturer's instructions (Fast Digestion of DNA, Thermo Scientific). DNA fragments were separated by 1% agarose gel electrophoresis, and fragment size analyzed to confirm proper insertion.

2.2.1.3 Agarose DNA gel electrophoresis

DNA gel electrophoresis was performed on 0.8% or 1% agarose gels in TAE buffer. Samples were mixed with LD (loading dye) (Thermo Scientific) before loading onto gel. The 0.8% gels were run on 50 V (for better resolution of bands in gel) and 1% gels on 100 V for 20-30 min (Run One Electrophoresis Cell, Embi Tec), and were visualized by UV light after soaking the gel in 10 ng/l ethidium bromide and recorded by digital camera (Kodak EDAS 290, exposition 2 s).

2.2.1.4 DNA gel and PCR purification

After gel electrophoresis, bands of interest (insert or linearized vector) were excised from gel under 70% UV light and purified. The protocol NucleoSpin Gel and PCR Clean up (Macherey-Nagel, Clontech) for DNA extraction from agarose gels and PCR Clean up was followed. Briefly, twice the amount the weight of the gel or volume of the PCR solution NTI Buffer was added. To melt the gel, samples were incubated for 10 min at 50 °C (PCR Clean up procedure skipped this step). The samples were centrifuged 30 s at 11 000 *g* (Centrifuge 5415 R, Eppendorf), washed with NT3 Buffer and centrifuged twice at same conditions. The columns were centrifuged again for another 2 min then incubated for 3 min at 70 °C. The elution step was divided into two steps to increase DNA recovery. NE Buffer (15 µl), warmed to 70 °C, was added and incubated, for shorter fragments (<1000 bp) on RT, for larger (>1000 bp) on 70 °C for 15 min. This step was repeated twice. Purified fragments were separated and visualized by 1% agarose gel electrophoresis. Concentrations of purified inserts and linearized vectors were measured using Nanodrop 1000 Spectrophotometer (Thermo Scientific, V3.8.1 program) and stored at -20 °C.

2.2.1.5 Dephosphorylation of plasmid DNA

To prevent unwanted plasmid recircularization after restriction digestion, dephosphorylation of 5' sticky ends of linearized plasmid was performed by a phosphatase (Shrimp Alkaline Phosphatase, 1 U/µl; Cat. No. 11758250001, Roche) per manufacturer's instructions. The reaction was heated to 37 °C and incubated for 10 min which was followed by purification procedure and concentration measurement as described in section 2.2.1.4.

2.2.1.6 Cloning procedures

2.2.1.6.1 Ligation reaction

Ligation reffers to the pocess of joining two compatible DNA fragments through the action of a ligase by forming a phosphodiester bond between 3' and 5' ends. Thus, both the gene to be inserted, and the target vector had to be digested with the same or compatible RE. The ligation reaction was prepared with 50 ng linearized and purified plasmid, and 50 ng of gene insert. T4 ligase (2 Weiss U) (Thermo Scientific, 5 Weiss U/µl) and appropriate buffer were used. Final volume was 30 µl (prepared in 0.2-ml tube) and fragments were ligated at 22 °C overnight. This solution was used directly for transformation procedures.

2.2.1.6.2 In-Fusion reaction

The In-Fusion cloning technology is based on a 3' exonuclease which generates single-stranded 5' overhangs at the termini of linear double-stranded DNA. DNA fragments are then annealed via complementary 15-bp overlaps at the termini of the insert and a linearized vector. These 15-bp long 5' extensions homologous to target vector were engineered by designing primers for gene amplification (**Table 1**) which also contained restriction sites for corresponding restriction endonucleases. After gene amplification by PCR and purification, the In-Fusion reaction was carried out per protocol In-Fusion® HD Cloning Kit User Manual. In a total volume of 10 µl, 50 ng of linearized plasmid vector and 25 ng of insert were mixed. The solution was incubated for 15 min at 50 °C. The recombinant circular constructs were then rescued in *E. coli.*

2.2.1.7 Transformation of competent *E. coli* cells

E. coli competent cloning and expression strains were transformed via heat shock according to manufacturer instruction. Briefly, 1 µl of initial or target vector, or 2.5 µl of ligation or In-fusion reaction was mixed with 50 µl thawed competent cells in a 14-ml round-bottom Falcon tube or in a 1.5-µl Eppendorf tube on ice and incubated for 30 min. The C2987H cells were heat shocked for 30 s at 42 °C, the XL10 Gold and Stellar™ cells for 45 s, and Rosetta™ for 90 s. The cells were then incubated 5-8 min on ice, SOC medium warmed to 37 °C added to the total volume of 0.5 ml and mixture was incubated for 1 h at 37 °C (250-

300 rpm). A volume of 50-100 µl of bacterial suspension was plated on selective LB plates with appropriate antibiotic (**Table 3**) and were grown overnight at 37 °C. XL 10 Gold strain was transformed with corresponding empty vectors serving as negative control to exclude false positives. Single bacterial colonies (up to 10) were picked and immersed to 3 ml liquid LB medium supplemented with appropriate antibiotic. Bacterial suspension were incubated overnight at 37 °C (250-300 rpm), and further used for colony screening, plasmid isolation or glycerol stocks preparation.

2.2.1.8 Colony screening by PCR

A portion of overnight bacterial suspension (200 µl) was centrifuged at 14 000 *g*, for 2 min. The pellet was resuspended with 200 µl sterile water and heated to 95 °C for 5 min. The lysed solution (2 µl) served as template and was added to a PCR mixture of 25 µl in a 0.2-ml reaction tube per manufacturer's instructions (EmeraldAmp® MAX PCR Master Mix, Takara). Gene specific forward and reverse primer (**Table 1**) were added (5 pmol). A negative control (distilled water) and positive control (a construct containing the insert) were prepared in parallel. PCR was carried out in Gene Amp PCR System 2700 (Applied Biosystems). Initial denaturation step was performed at 98 °C for 3 min, followed by 40 cycles of denaturation at 98 °C for 10 s, annealing at 55 °C for 30 s, extension at 72 °C for 1 min/kb and a final extension step at 72 °C for 7 minutes. Amplified inserts were resolved and visualized on 1% agarose gel.

2.2.1.9 Glycerol stock preparation

Glycerol stocks were prepared by mixing 500 µl 100% glycerol and 500 µl transformed XL 10 Gold bacterial suspensions in a 1.5 ml tube under sterile conditions. Stocks were frozen in liquid nitrogen and stored at -80 °C.

2.2.1.10 Plasmid isolation

For the isolation and purification (miniprep) of plasmid DNA the Wizard® Plus SV Minipreps DNA Purification System protocol was followed with few alternations. A volume of 2 ml of overnight bacterial suspension was centrifuged at room temperature (RT), 14 000 *g* for 5 min (Centrifuge 5451C, Eppendorf). The pellet was resuspended with provided Cell Resuspension Solution. Then, Cell Lysis Solution, Alkaline Protease Solution and Neutralization Solution were added (after each addition, the tubes were inverted a few times). The tubes were centrifuged for 10 min and the cleared lysate was decanted into the Spin Columns on top of the Collection Tubes. After spinning the samples for 1 min, Wash Solution was added twice and centrifuged for 1-2 min. The flow through was always discarded. The Spin Column was than transferred to a sterile 1.5 ml microcentrifuge tube. In the elution step, 50 µl Nuclease-Free Water was added to the Spin Column and incubated for 15 min at 37 °C and then centrifuged for 5 min. This step was repeated once more. To verify the presence of DNA, gel electrophoresis in 1% agarose gels was performed. DNA samples were stored at -20 °C. Plasmids were verified by restriction digestion and sequencing.

2.2.1.11 Insert verification by sequencing

To analyze inserts sequence accuracy, two representative DNA samples of each final construct (15 µl) were sequenced in service (Macrogen Europe, The Netherlands) with universal commercial primers from Macrogen. Sequences were analyzed in Clustal X (Larkin et al., 2007).

2.2.2 PROTEIN EXPRESSION AND PURIFICATION

2.2.2.1 Verification of protein synthesis in *E. coli*

After the final constructs were transformed to *E. coli* expression strain, verification of protein overexpression was carried out. For verification purposes, 800 µl of overnight bacterial suspension was added to 15 ml LB medium suplemented with appropriate antibiotics. Bacterial suspensions were incubated at 37 °C at 250-300 rpm until its optical density at 600 nm (OD_{600}) reached at least 0.6 (Ultrospec 10, Cell Density Meter, Amersham Biosciences). Bacteria were induced with 1 mM isopropyl β-D-1-thiogalactopyranoside (IPTG; Biochemica, AppliChem CmBH) and incubated for 3 h at 37 °C and 150 rpm. Induced bacterial suspensions (1 ml) were centrifuged at 4 °C, 4000 *g* for 5 min, the pellet resuspended in 100 µl 5× SB buffer and incubated for 5 min at 95 °C. SDS-PAGE, western blotting and immunodetection were performed as described in section 2.2.2.4. The remaining 14 ml were used for purification protocol optimization.

2.2.2.2 Preparative protein overexpression in *E. coli*

For purification purposes, 200 ml of liquid LB medium suplemented with appropriate antibiotics was inoculated with 2-3 ml of overnight *E. coli* suspension. Bacterial suspensions were incubated at 37 °C at 250-300 rpm until its optical density at OD_{600} reached at least 0.6. IPTG was added to a final concentration of 0.5-1 mM. The cultures were then incubated for 3-4 h at 37 °C or 16 h at 15 °C, at 150 rpm. The cells were collected by centrifugation at 4000 *g* for 5 min, washed with 1× PBS or 50 mM Tris-HCl (pH 8) buffer and after centrifugation, the pellets were frozen in liquid nitrogen and stored at -80 °C.

2.2.2.3 Protein extract preparation

All steps were prepared on ice with cold buffers. Thawed bacterial pellets were resuspended with lysis buffer (section 2.1.7.4). The cells were disrupted by sonication with 6-10 ten-second bursts at 200-300 W and 30 s cooling periods in between (Bioblock Scientific, Vibracell™). The cell lysate was clarified by centrifugation at 4 °C, 20 000 *g* for 20 min and the supernatant filtered through 0.45 µm filters (Minicare Bio-Start®, Sartorius Stedium Biotech SA, 16555). Resulting protein extract was used for protein purification.

2.2.2.3.1 Purification of 6× His-tagged proteins

Ni-NTA agarose (QIAGEN GmBH) was equilibrated with His lysis buffer. Protein extract was added to 100-200 µl Ni-NTA agarose beads. After overnight incubation in 15 ml-Falcon tubes at 4 °C by mixing and subsequent bead precipitation (4 °C, 500 *g*, 5 min) supernatant (flow through) was removed and beads were transferred to a 1.5 ml-tube. Beads were washed with a series of buffers with decreasing salt concentrations (W1-W3). Each washing buffer was added twice (2× 1 ml), incubated on beads for 5-10 min and removed by centrifugation (4 °C, 800 rpm, 1 min). In some cases, an alternative approach was carried out where washing was performed in 15 ml-Falcon tubes with 5-10 ml portions of W1 and W2 buffer, 5-10 min incubation step and centrifugation (4 °C, 500 *g,* 1 min). The last washing step, with 1-2 ml W3, and all elution steps were performed on filter columns. Fusion proteins were eluted in three steps: twice with 200 µl elution buffer and once with 300 µl of 2 M imidazole. After each addition, the samples were incubated 10 min at 4 °C. Samples (50 µl) of protein extract, pellet, flow through, and washes were collected. Only 15-20 µl of eluted fusion protein was used for detection. As the pull-down assay was to be performed in 1× PBS buffer, Tris buffer was replaced with 1× PBS. All three protein elutions were mixed and buffer was replaced using Amicon® Ultra-4 Centrifugal Filter Devices (Merck Millipore Sigma) and centrifugation (4 °C, 3500 *g*, 5-20 min). Proteins were stored at 4 °C with the addition of 0.02% sodium azid for short-term storage or at -20 °C with the addition of 10% glycerol for long-term storage.

2.2.2.3.1.1 Additional purification of 6× His-tagged proteins

To minimize unwanted protein contaminations, a second purification procedure was performed. For this purpose, all three protein elutions from the first affinity chromatography were mixed and buffer was replaced with replacement buffer (50 mM Tris-HCl pH 8, 300 mM NaCl, 30 mM imidazole, 1 mM β-met) using Amicon® Ultra-4 Centrifugal Filter Devices as described in section 2.2.2.3.1. Fresh Ni-NTA resin (100 µl) was added to the 1.5 ml-protein solution in 1.5-ml tubes and incubated overnight at 4 °C by mixing and washed as previously explained. The elution steps were performed in 0.35 µm Mobicols columns (MoBiTec, Molecular Biotechnology, M2135). Samples (50 µl) of flow through and washes

were collected. Only 15-20 µl of eluted fusion protein was used for detection. Buffer was replaced with 1× PBS and proteins were stored at 4 °C with the addition of 0.02% sodium azid for short-term storage or at -20 °C with the addition of 10% glycerol for long-term storage.

2.2.2.3.2 Purification of GST-tagged proteins

Protein extract was applied to 100-200 µl Glutathione Sepharose™ 4B, (GE Healthcare Bio-Sciences AB) that was equilibrated in the GST lysis buffer before use. The solution was incubated overnight in 50 ml-Falcon tubes at 4 °C by mixing followed by centrifugation (4 °C, 500 *g*, 5 min). Supernatant (flow through) was removed and sepharose transfered to a 1.5 ml-tube, after which the beads were washed 3-5 times with 1 ml 1× PBS buffer. In some cases 1× PBS was supplemented with 0.05% Tween 20. If needed, more effective purification was performed by adding 0.5-1 M NaCl. The beads were then washed with pure 1× PBS to avoid high salt concentrations. Each time beads were precipitated by centrifugation (4 °C, 800 rpm, 1 min). After the last wash, remaining washing buffer was completely removed by an insulin syringe and fresh 1× PBS (100-150 µl) was added. GST-tagged proteins were kept on beads. During purification, 50 µl portions of protein extract, bacterial pellet, flow through, and washes were collected. For detection of purified protein (still attached to beads) 15 µl were used. Purified proteins attached to beads were stored at 4 °C.

2.2.2.4 Protein detection

2.2.2.4.1 SDS-PAGE and in gel protein staining

Protein visualizations were carried out by sodium dodecyl sulfate (SDS) polyacrylamide gel electrophoresis (PAGE) in 10%, 4-12% or 12% SDS Precast Gels (NXG01212, RunBlue, Expedeon). Protein samples were incubated at 95 °C after 5× SB buffer addition, and a volume of 10-30 µl was loaded on gel. The gels were run in 1× SDS RunBlue buffer (TEO-Tricine-SDS, Expedeon) 30-60 min at 100 V, and then 2 h at 200 V (DCX-700 CBS Scientific). After electrophoresis proteins in gel were stained with Coomassie Brilliant Blue (CBB)-based solution (Instant Blue®, Expedeon) by mixing for 15-30 min.

2.2.2.4.2 Western blotting and immunodetection

After electrophoresis proteins were electroblotted on a polyvinylidene membrane (PVDF; Transfer Membranes, Immobilon®-P) according to Dual Cool Electrophoresis System instructions (Mini-vertical Slab Gel Blotting System, DCX-700, CBS Scientific). The assembled core (membrane, gel, filters and sponges) was immersed into transfer buffer and blotting was performed overnight at RT at 12 V. Membranes were blocked in 2% non-fat milk (prepared in 1× PBS) for 7-8 h and afterwards incubated with mouse monoclonal anti-6× His (Roche 11922416001) or mouse monoclonal anti-GST (Sigma-Aldrich® SAB4200692) antibody diluted 1:1000 in 2% non-fat milk (prepared in 1× PBS) at 4 °C overnight. Secondary antibody (Anti-Mouse IgG Peroxidase Conjugate, Sigma A4416) diluted 1:5000 in 2% non-fat milk (prepared in 1xPBS) was added on membranes and incubated 2-3 h at room temperature. After each antibody, membrane was washed three times with 1× PBS for 10 min. Finaly, 500 µl of HRP substrate (Luminata™ Forte HRP Substrate, Millipore) was pipetted on the membranes (protein-side up) and incubated for 1-2 min. Inside a dark room, films were carefully leaned against drained membranes (covered in clean sheet protector) and incubated, depending on the intensity of the reaction, for 1-15 min. The film was developed using 15% developer (Heraeus Kulzer GmBH) and 15% fixer (Heraeus Kulzer GmBH) solutions respectively.

2.2.3 PULL-DOWN ASSAY

The pull-down assay is an *in vitro* method for physical protein interaction analysis that includes a protein of interest (bait) and the potential interacting partner (prey). It is used for confirming or identifyng new interactions. While bait proteins are immobilized to a matrix, prey proteins are present in a solution that is added to the matrix. After incubation and washing, attached proteins are visualized by CBB staining and immunodetection. Here, BPM1 protein interactions were examined by two types of pull-down assay. One to one pull-down assay was used to examine BPM1-RDM1 interaction. In one to two pull-down assays BPM1 was bait and, RDM1 and DMS3; RDM1 and HB6; or DMS3 and HB6 were preys.

Prior to pull-down assay, samples of purified prey proteins in 1× PBS buffer (15 µl) were run on SDS-PAGE and stained with CBB. The optical density was estimated by using ImageJ (National Institutes of Health; http://rsb.info.nih.gov/ij/download.html). Based on these, the volumes of prey protein for pull-down assay were defined.

To examine protein-protein interactions, bait to prey and bait to two preys reactions were performed. Appropriate negative controls with either glutathione S-transferase loaded on glutathione sepharose beads (GST) (provided for these experiments), as well as glutathione sepharose with unbound proteins (GSH) were used (2 µl). The reactions were carried out in a total volume of 0.5 or 1 ml 1× PBS in 1.5 ml-tubes. Regardless of concentration, 15 or 30 µl of GST-tagged protein (bait) attached to beads and 8-100 µl of His-tagged prey protein was added to mixture. The reactions were incubated overnight at 4 °C by rotation. Beads were precipitated by centrifugation and washed three times with 1 ml 1× PBS. Finally, all residual buffer was removed by an insulin syringe, the beads resuspended with 5× SB and incubated at 95 °C for 5 min. Samples were resolved by SDS-PAGE and visualized by immunodetection using anti-His antibody. The same membrane was stained with CBB.

3 RESULTS

3.1 PLASMID CONSTRUCTS FOR PROTEIN EXPRESSION

The first aim of this thesis was the construction of expression vectors suitable for overexpression of *A. thaliana* proteins in *E. coli*. All constructs for protein expression were successfully designed (**Figures 5-9**). Genes were cloned into the multiple cloning site (MCS) of plasmid vector in frame with N-terminal 6× His or GST tag. Gene incorporation was verified by restriction digestion. To verify the sequence accuracy of incorporated genes, two representative replicas from each construct were sequenced.

3.1.1 pGEX4T1-DMS3 construct

DMS3 gene was amplified by PCR on pB7WGF-DMS3 template using InF_DMS3_Fw and InF_DMS3_Rev primers (**Table 1**). The pGEX4T1 target vector was linearized by restriction digestion with BamHI and EcoRI enzymes. Both *DMS3* and pGEX4T1 fragments were purified and subjected to In-Fusion reaction. Resulting DNA fragments of insert and plasmid with 5' single strand overhangs were transformed into competent bacteria strain Stellar^{TM} where pGEX4T1-DMS3 was regenerated (**Figure 5**). Transformed bacteria were selected on LB medium with ampicillin (Amp) and colony screening was performed by PCR. From overnight cultures plasmids were isolated. Presence of *DMS3* gene in recombinant pGEX4T1-DMS3 plasmid was confirmed by restriction digestion by BamHI and EcoRI enzymes resulting in fragments of 1269 bp and 4960 bp (**Figure 5A**). Undigested plasmid of 6229 bp was detected. DNA sequence was verified by sequencing.

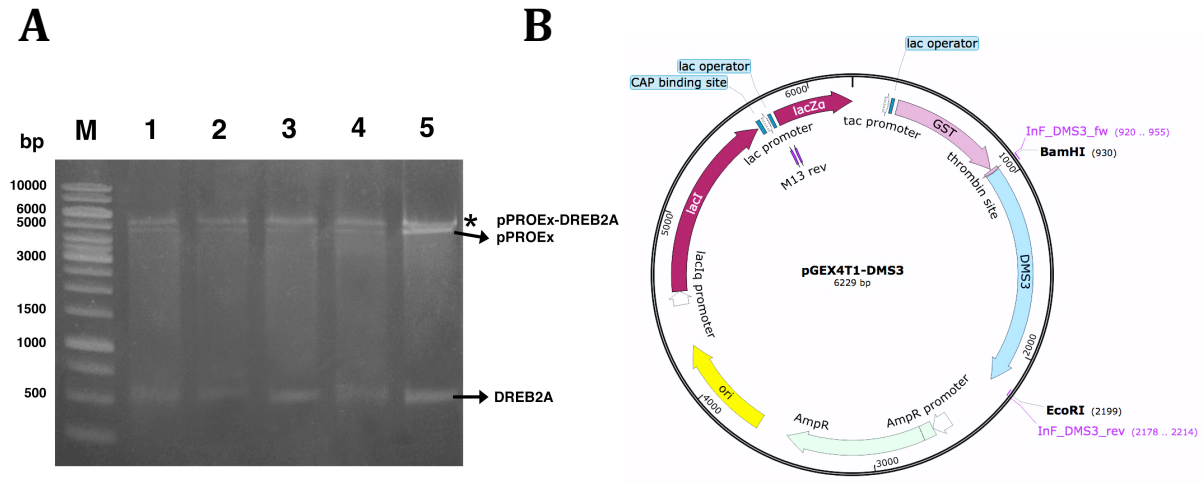

Figure 5. Restriction verification of pGEX4T1-DMS3 construct **(A)** and its plasmid map obtained in SnapGene program **(B).** Recombinant pGEX4T1-DMS3 was digested with EcoRI and BamHI but the digestion was incomplete (undigested fragment is annotated with an asterisk, 6229 bp). Expected bands of *DMS3* insert (1269 bp) and pGEX4T1 vector (4960 bp) were detected (depicted with an arrow). M is Gene Ruler 1 kb DNA Ladder (Thermo Scientific). Individual minipreps are numbered as 1 and 2.

3.1.2 pPROEx-DREB2A construct

DREB2A gene was amplified via PCR with a provided sample of complementary DNA (cDNA) of *A. thaliana* as template using InF_DREB2A_Fw and InF_DREB2A_Rev primers (**Table 1**). Due to low amount of *DREB2A* products, another PCR reaction was performed, with the *DREB2A* PCR products of the first reaction serving as templates. Target vector pPROEx was linearized by EcoRI. After purification, *DREB2A* and pPROEx were directly subjected to In-Fusion reaction. DNA fragments of insert and plasmid with 5' single stranded overhangs were transformed into competent Stellar^{TM} strain for plasmid regeneration (**Figure 6**). Potential transformants were first screened via PCR. Presence of *DREB2A* insert was verified by restriction with EcoRI and BamHI (**Figure 6A**). BamHI cut within the gene sequence and fragments of 506 bp and 518 bp emerged which were visible on gel as one band. Linearized vector (4771 bp) and undigested vector (5795 bp) were detected. Sequence of insert was verified by sequencing.

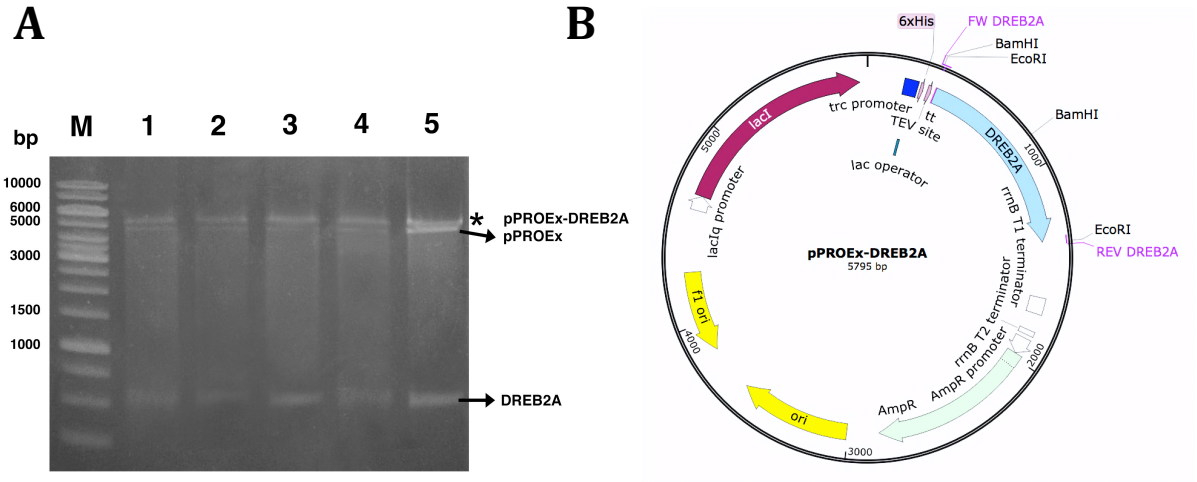

Figure 6. Restriction verification of pPROEx-DREB2A construct **(A)** and its plasmid map obtained in SnapGene program **(B).** Recombinant pPROEx-DREB2A was digested with EcoRI and BamHI but the digestion was incomplete (annotated with an asterisk, 5795 bp). Bands of *DREB2A* insert (506 and 518 bp) and pPROEx vector (4771 bp) became visible (depicted with an arrow). M is Gene Ruler 1 kb DNA Ladder (Thermo Scientific). Individual minipreps are numbered 1-5.

3.1.3 pPROEx-HB6 construct

HB6 gene was obtained by pGAD424-HB6 digestion with BamHI and XbaI, and *HB6* gene purified from agarose gel. Linearization of pPROEx-KAT target vector was performed with the same restriction enzymes. Both fragments were excised and purified from agarose gel. Restriction digestion of plasmid pPROEx-KAT with BamHI and XbaI (dual cutter) resulted in three DNA fragments, one of the linearized vector, and two shorter DNA fragments. To prevent religation, fragments were dephosphorylated by an alkaline phosphatase. The linearized dephosphorylated pPROEx was purified. *HB6* and pPROEx DNA fragments were ligated with T4 DNA ligase. Ligation mixture was transformed to C2987H cloning strain to regenerate recombinant plasmids (**Figure 7**). Transformed *E. coli* was selected on Amp plates and grown overnight in liquid medium. pPROEx-HB6 plasmids were isolated and inserts presence proved by restriction with BamHI and XbaI. DNA fragments of 946 bp and 4722 bp (**Figure 7A**), as well as sequencing proved accurate cloning of *HB6* into pPROEx.

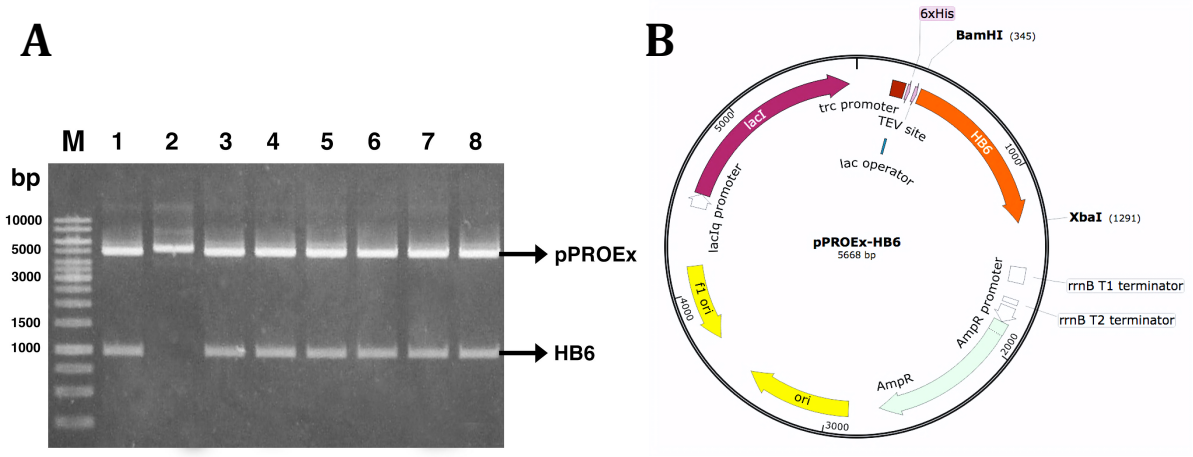

Figure 7. Restriction verification of pPROEx-HB6 construct **(A)** and its plasmid map obtained in SnapGene program **(B).** Recombinant pPROEx-HB6 was digested with BamHI and XbaI. Only two observed bands indicated complete digestion. Expected bands of *HB6* insert (946 bp) and pPROEx vector (4722 bp) became visible (depicted with an arrow). M is Gene Ruler 1 kb DNA Ladder (Thermo Scientific). Individual minipreps are numbered 1-8. Colony in lane 2 most likely contains an unrestricted plasmid vector.

3.1.4 pET28a-RDM1 construct

Initial vector pGAD424-RDM1 and target vector pET28a were digested with EcoRI and HindIII to obtain *RDM1* gene and linearized pET28a respectively. After agarose gel electrophoresis, both fragments were excised and purified from gel. Vector pET28a and *RDM1* gene were subjected to ligation reaction. Recombinant plasmids were transformed to C2987H cloning strain for recombinant plasmid regeneration (**Figure 8**) and were selected on kanamycin (Kan) LB plates. Overnight liquid cultures were grown and pET28a-RDM1 was isolated. Insert was verified by restriction with EcoRI and HindIII resulting in fragments of 744 bp and 5350 bp (**Figure 8A**) and sequencing.

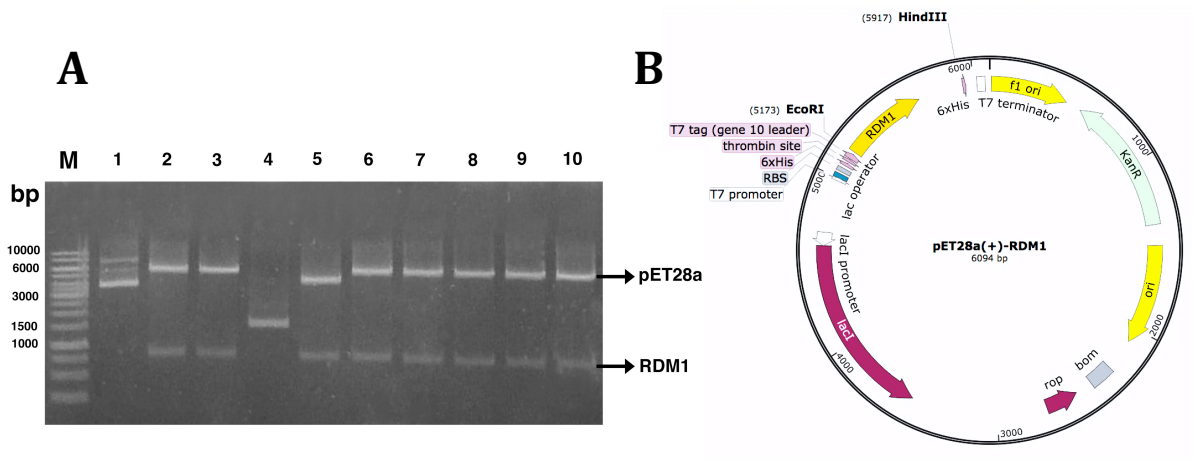

Figure 8. Restriction verification of pET28a-RDM1 construct **(A)** and its plasmid map obtained in SnapGene program **(B).** Recombinant pET28a-RDM1 was digested with EcoRI and HindIII and the digestion was complete. Bands of *RDM1* insert (744 bp) and pET28a vector (5350 bp) became visible (depicted with an arrow). M is Gene Ruler 1 kb DNA Ladder (Thermo Scientific). Individual minipreps are numbered 1-10. Colonies 1 and 4 did not contain desired plasmid.

3.1.5 pPROEx-WRI1 construct

WRI1 gene was amplified by PCR with pCR8-WRI1 serving as template and InF_WRI1_Fw and InF_WRI1_Rev primers (**Table 1**). Target vector pPROEx-KAT was digested with EcoRI and BamHI. Purified *WRI1* and pPROEx were cloned using In-Fusion method. DNA fragments of insert and vector with 5' single strand overhangs were transformed into competent *E. coli* strain Stellar^{TM} for plasmid regeneration (**Figure 9**). After bacterial selection on Amp LB plates, plasmids were isolated from bacterial suspension and presence of *WRI1* in recombinant pPROEx-WRI1 plasmid was proved by restriction digestion with EcoRI and BamHI (**Figure 9A**) and sequencing. The chosen EcoRI cut within the gene sequence, and as a consequence, two fragments (one of 1054 bp and the other of 269 bp) emerged, along with the linearized vector of 4772 bp. The smallest band was invisible due to its size.

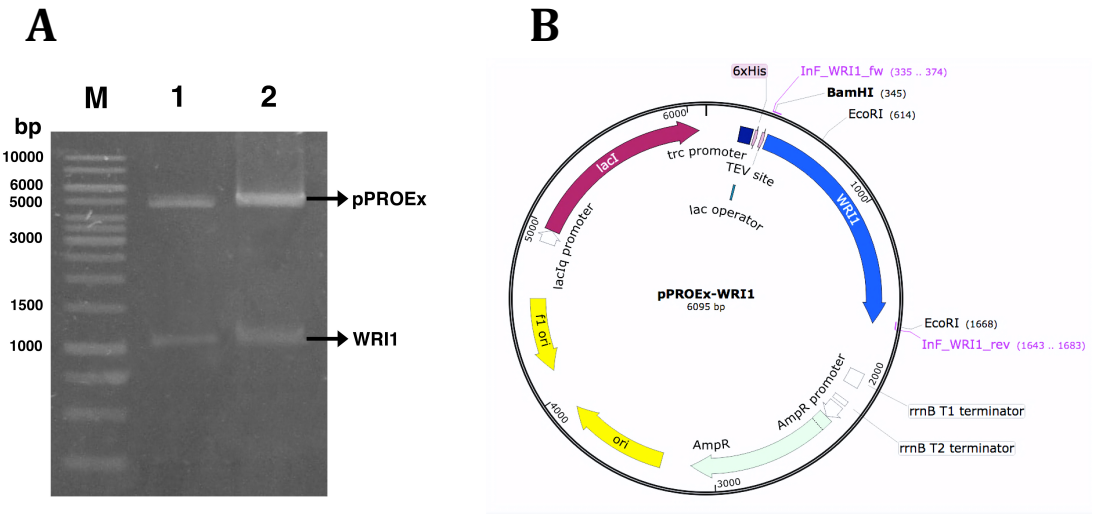

Figure 9. Restriction verification of pPROEx-WRI1 construct **(A)** and its plasmid map obtained in SnapGene program **(B).** Recombinant pPROEx-WRI1 was digested with EcoRI and BamHI and the digestion was complete. Bands of *WRI1* insert (1054 bp) and pPROEx vector (4772 bp) became visible (depicted with an arrow). M is Gene Ruler 1 kb DNA Ladder (Thermo Scientific). Individual minipreps are numbered as 1 and 2.

3.2 FUSION PROTEIN OVEREXPRESSION AND PURIFICATION

After gene cloning, all recombinant expression plasmids were transformed into Rosetta™ *E. coli* strain for protein expression verification. Transformed bacteria were selected on plates containing, apart from ampicillin (Amp) or kanamycin (Kan), chloramphenicol (Chl) for selection of the pRARE plasmid (a plasmid carrying rare eukaryotic tRNA genes) present in Rosetta™ strain. Protein expression was induced by IPTG and verification performed by SDS-PAGE, CBB staining (**Figure 10A**) and immunodetection (**Figure 10B**). Similar protocols were followed when expressing proteins for preparative purposes. Numerous repetitions and various alternations to the protein induction protocols failed to obtain DREB2A-His and soluble WRI1-His fusion proteins.

After verifying protein overexpression in *E. coli*, proteins were expressed in a larger volume (200 ml) of cell culture to gain fusion proteins in sufficient quantities for preparative purification purposes and pull-down reaction. After protein synthesis induction, bacteria were centrifuged, washed, resuspended in lysis buffer and disrupted by sonication. Proteins were extracted and tagged proteins purified. Amount and purity of recombinant proteins depended on their size and fusion tag. The greater the size, the smaller the amount of protein obtained. GST-tagged proteins were better purified than 6× His-tagged proteins due to reduced unspecific binding. Samples of supernatant (protein extract after cell lysis and centrifugation), bacterial pellet (residual pellet after cell lysis and centrifugation), flow through (unbound proteins), washes, elutions (purified protein samples) and Ni-NTA resin (resuspended beads after elutions) or glutathione beads (with proteins still attached to them) were loaded on gel to follow purification procedure. In the ideal case, the desired band was expected to be found in supernatant, and a purified version in elution lane, but not in pellet, flow through, wash or bead lanes.

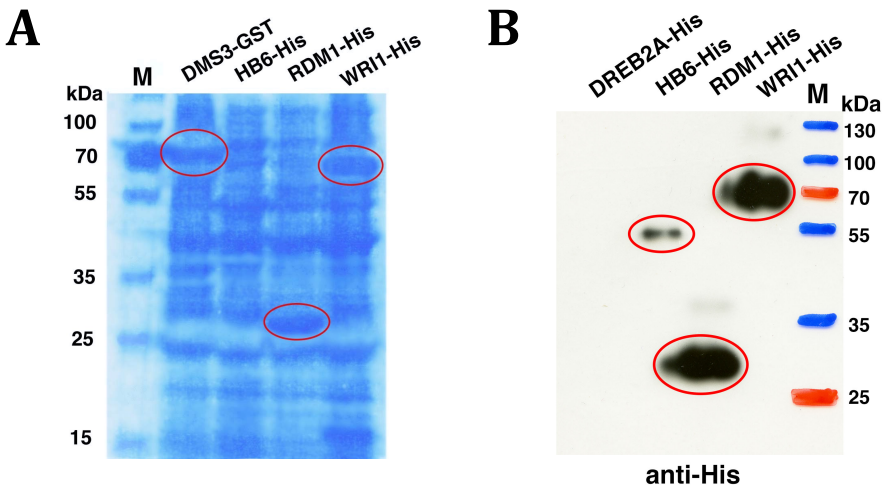

Figure 10. (A) Verification of DMS3-GST, HB6-His, RDM1-His and WRI1-His protein overexpression (circled in red) after SDS-PAGE and CBB staining. Only HB6-His could not be discerned. **(B)** DREB2A-His, HB6-His, RDM1-His and WRI1-His fusion proteins after immunodetection with anti-His antibody (circled in red). DREB2A-His was not detected. HB6-His signal was observed only after immunodetection. Fusion proteins WRI1-His and RDM1-His showed a very high protein yield. Almost all proteins show shift in gel, since theoretical molecular weight are 38.4 kDa for HB6-His, 22.4 kDa for RDM1-His, 52.7 kDa for WRI1-His and 73 kDa for DMS3-GST. M is Page Ruler^{TM} Plus Prestained Protein Ladder (Thermo Scientific).

3.2.1 BPM1-GST protein overexpression and purification

The protocol for BPM1-GST protein expression and purification has been developed previously and repeated here as follows. pGEX4T1-BPM1 recombinant plasmid was transformed into *E. coli* expression strain Rosetta^{TM} and selected on LB plates containing Amp and Chl. From overnight bacterial suspension, 200-ml culture for protein induction was made. Culture was incubated at 37 °C and 300 rpm until its optical density reached at least 0.6. Protein expression was induced with 0.5 mM IPTG and incubated for 16 h at 15 °C and 150 rpm. The bacterial suspension was centrifuged and pellet washed with 1× PBS. The bacterial pellet was resuspended in 20 ml lysis (extraction) GST buffer 2 and was lysed on ice with 8 ten-second sonication bursts. The lysate was clarified by centrifugation and filtration, and 200 µl glutathione sepharose beads, previously equilibrated in GST lysis buffer 2, was added to supernatant. The suspension was incubated overnight at 4 °C and washed in 1× PBS supplemented with 0.05% Tween 20. Additional washing was performed with 1× PBS containing 1 M and 0.5 M NaCl. BPM1-GST fusion protein was detected by SDS-PAGE and CBB staining (**Figure 11**). Increased salt concentrations in buffer resulted in purer BPM1-GST but concentration of protein decreased significantly (**Figure 11**). BPM1-GST and GST showed a slight shift in SDS-PAGE when comparing the position on gel to their theoretical values of 71 kDa and 26 kDa respectively. A great amount of fusion protein was found in pellet (P) most likely due to insufficient cell lysis by sonication or BPM1-GST aggregate formation. BPM1 showed two isoforms on gel (double bands in P, B, B_1) noted with an asterisk. Taken together, BPM1-GST was purified in sufficient quantities and purity to enter pull-down assay.

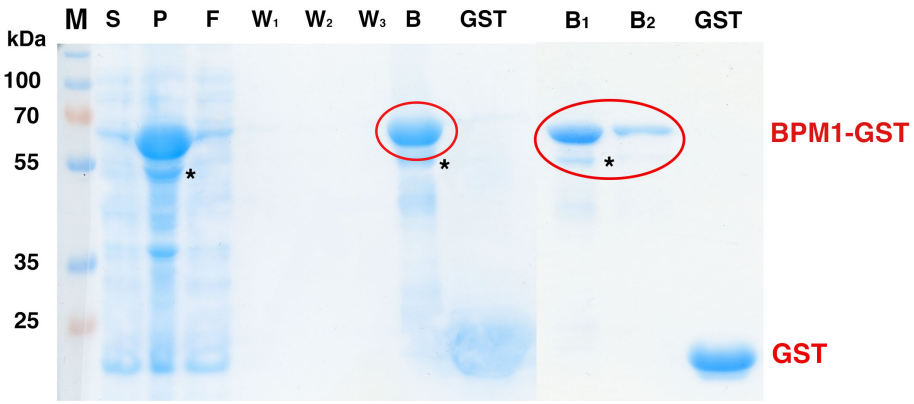

Figure 11. BPM1-GST protein detection after SDS-PAGE and CBB staining (circled in red). Theoretical molecular weight for BPM1-GST is 71 kDa, and here it is detected at 60 kDa. Samples from left to right: supernatant (S), pellet (P), flow through (F), washes (W_1-W_3), uneluted BPM1-GST (B) and GST only. Additional purified BPM1-GST is in B_1 and B_2. Fusion protein was found in pellet (P) due to insufficient cell lysis or protein aggregation. The asterisk indicates the BPM1 isoform. M is Page Ruler^{TM} Plus Prestained Protein Ladder (Thermo Scientific).

3.2.2 DMS3-His protein overexpression and purification

The protocol for DMS3-His protein expression and purification has been developed previously and repeated here as follows. pET28a-DMS3 recombinant plasmid was transformed into *E. coli* expression strain Rosetta^{TM} and selected on LB plates containing Kan and Chl. From overnight bacterial suspension, preparative culture for protein induction (200 ml) was made with the same antibiotics and incubated at 37 °C and 300 rpm until its optical density reached at least 0.6. Protein expression was induced with 1 mM IPTG and incubated for 3 h at 37 °C and 150 rpm. The bacterial suspension was centrifuged and pellet washed with 50 mM Tris-HCl pH 8. Bacterial pellet was resuspended in 15 ml His buffer and was lysed on ice with 8 ten-second sonication bursts. The lysate was clarified by centrifugation and filtration, and 200 µl Ni-NTA resin, previously equilibrated in His lysis buffer, was added. The suspension was incubated overnight at 4 °C and washed in a series of buffers (W1-W3) in an alternative purification approach described in section 2.2.2.3.1. DMS3-His fusion protein was detected by SDS-PAGE and CBB staining (**Figure 12**). Position on gel corresponded with its theoretical molecular weight (Mw) of 49 kDa. Fusion protein was partially detected in pellet (P) due to insufficient cell lysis or protein agregation

(**Figure 12**). Elution was incomplete as fusion proteins were detected in sample containig resuspended beads after protein elution (lane B). Regardless, DMS3-His showed sufficient purity and amount to continue with pull-down experiment.

3.2.3 DMS3-GST protein overexpression and purification

pGEX4T1-DMS3 recombinant plasmid was transformed into *E. coli* expression strain Rosetta^{TM}. For DMS3-GST protein production, one random bacterial colony was inspected. From overnight bacterial suspension culture for protein induction was made with addition of Amp and Chl and incubated at 37 °C and 300 rpm until its optical density reached at least 0.6. For verification purposes, protein expression was induced with 1 mM IPTG and after incubation for 3 h at 37 °C and 150 rpm, whole proteins were extracted and visualized by SDS-PAGE, CBB staining (**Figure 10A**), and immunodetection (data not shown). Majority of protein was present in bacterial pellet, so for preparative protein purification larger suspension volume (200 ml) was used. The same procedure as described above was followed. Induced bacterial suspension was centrifuged and washed with 1× PBS. Bacterial pellet was resuspended in 20 ml GST lysis buffer 1, lysed on ice with 10 ten-second sonication bursts. The lysate was clarified by centrifugation and filtration after which 100 µl equilibrated glutathione sepharose beads was added. The suspension was incubated overnight at 4 °C and was washed with 1× PBS. DMS3-GST fusion protein was detected by SDS-PAGE and CBB staining (**Figure 13**). CBB-stained gel revealed little but pure fusion protein and a great amount of fusion protein was detected in pellet (P) due to insufficient cell lysis or protein aggregation. Position on gel corresponded with its theoretical Mw of 73 kDa. DMS3-GST, though initially a part of the planned experiment with reverse tags pull-down reaction (BPM1-His with GST-tagged other proteins), will be used in future pull-down experiments after BPM1-His protein purification.

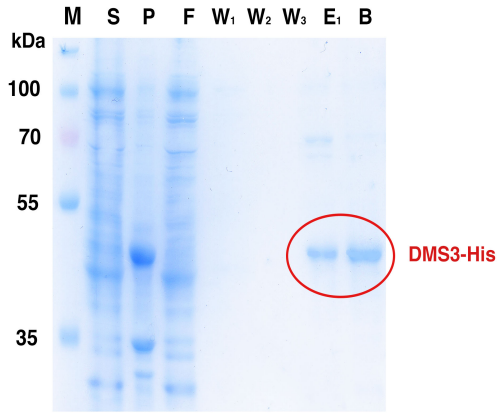

Figure 12. DMS3-His protein detection after SDS-PAGE and CBB staining (circled in red). Theoretical molecular weight for DMS3-His is 49 kDa. Samples from left to right: supernatant (S), pellet (P), flow through (F), washes (W_1-W_3), mixed elutions (E_1), resuspended beads (B). Fusion protein was found in pellet (P) due to insufficient cell lysis or protein aggregation. Lane B indicates incomplete protein elution. M is Page Ruler^{TM} Plus Prestained Protein Ladder (Thermo Scientific).

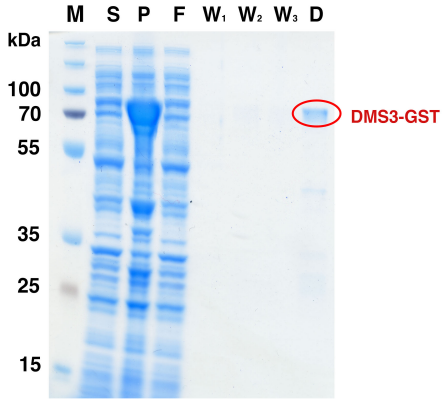

Figure 13. DMS3-GST protein detection after SDS-PAGE and CBB staining (circled in red). Theoretical molecular weight for DMS3-GST is 73 kDa. Samples from left to right: supernatant (S), pellet (P), flow through (F), washes (W_1-W_3) and uneluted DMS3-GST (D). Fusion protein was found in pellet (P) due to insufficient cell lysis or protein aggregation. M is Page Ruler^{TM} Plus Prestained Protein Ladder (Thermo Scientific).

3.2.4 DREB2A-His protein overexpression

pPROEx-DREB2A recombinant plasmid was transformed into *E. coli* expression strain Rosetta^{TM}. Initially, for DREB2A-His protein production verification, one random bacterial colony was inspected. For this purpose bacteria were grown on selective LB plates containing Amp and Chl. From overnight bacterial suspensions, cultures for protein induction were made containing the same antibiotics and incubated at 37 °C and 300 rpm until its optical density reached at least 0.6. For verification purposes, protein expression was induced with 1 mM IPTG and after incubation for 3 h at 37 °C and 150 rpm, whole proteins were extracted and visualized by SDS-PAGE, CBB staining (data not shown), and immunodetection (**Figure 10B**). No expression of DREB2A-His was detected. To overcome this problem several alternations in protocols for protein induction were made. Several bacterial colonies (5-10) from selective LB plates were screened by PCR (data not shown) and picked for protein production verification. Attempts were made with different volumes

of bacterial suspension and flasks in which bacteria were incubated. Different incubation temperatures of 20 °C, 30 °C and 37 °C for 16 h and 37 °C for 3 h or 1:30 h, at 150 rpm were tested. IPTG concentration for protein induction of 0.5 and 1 mM were tested. No DREB2A-His overexpression was observed.

3.2.5 HB6-His protein overexpression and purification

pPROEx-HB6 recombinant plasmid was transformed into *E. coli* expression strain Rosetta™. For HB6-His protein production one random bacterial colony was inspected. Bacteria were grown on selective LB plates containing Amp and Chl. From overnight bacterial suspension culture for protein induction were made containing the same antibiotics and incubated at 37 °C and 300 rpm until its optical density reached at least 0.6. Protein expression was induced with 1 mM IPTG. After 3 h incubation at 37 °C at 150 rpm, whole proteins were extracted and visualized by SDS-PAGE, CBB staining (**Figure 10A**) and immunodetection (**Figure 10B**). HB6-His was detected only after immunodetection and showed an elevated expression rate though in much smaller quantities than e.g. RDM1-His. To recover sufficient amount of protein, larger bacterial suspension volume (200 ml) was used for purification. The same procedure as described above was followed. Bacterial suspensions were centrifuged and washed with 50 mM Tris-HCl pH 8. Bacterial pellet was resuspended in 20 ml His buffer and lysed on ice with 9 ten-second sonication bursts. The lysate was clarified by centrifugation and filtration and 200 µl Ni-NTA resin, previously equilibrated in lysis buffer, was added. The suspension was incubated overnight at 4 °C and beads washed in a series of buffers (W1-W3). Protein elutions from the first purification step were subjected to a second purification as described in section 2.2.2.3.1.1 to reduce amounts of unspecificaly bound proteins. HB6-His fusion protein was detected by SDS-PAGE and CBB staining (**Figure 14**). HB6 showed two isoforms on gel (double bands in **Figure 14A**) noted with an asterisk. HB6-His showed a great shift in electrophoretic mobility since its theoretical Mw is 38.4 kDa. Elutions in **Figure 14A**, showed very impure fusion protein due to unspecific binding to Ni-NTA resin. After the second purification, much of the HB6-His was lost but the purity was high (**Figure 14B**). For that reason HB6-His had to be expressed and purified several times to reach the amount suitable for pull-down assay.

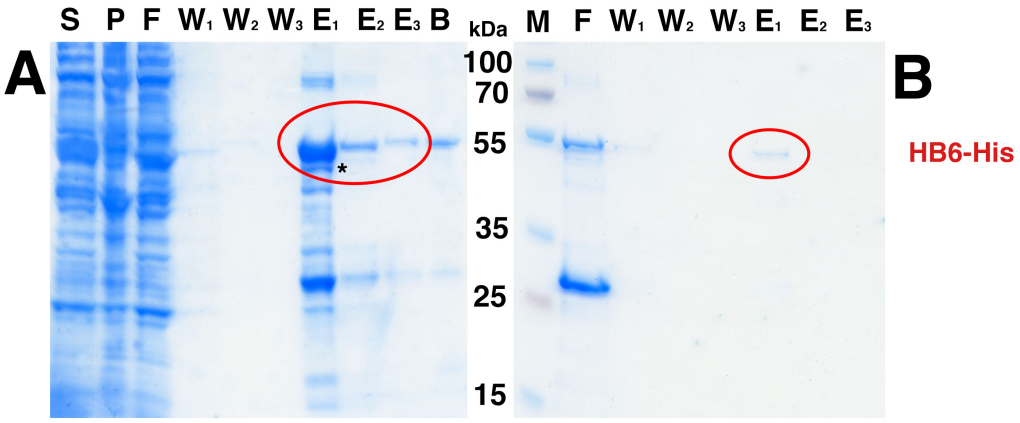

Figure 14. HB6-His protein detection after SDS-PAGE and CBB staining (circled in red). Theoretical molecular weight for HB6-His is 38.4 kDa, and here it is detected at 52 kDa. Samples from left to right: supernatant (S), pellet (P), flow through (F), washes (W_1-W_3), elutions (E_1-E_3), resuspended beads (B), after the first **(A)** and second **(B)** affinity chromatography. During additional purification much protein sample was lost but purity rose rapidly. The asterisk indicates a HB6 isoform. M is Page Ruler^{TM} Plus Prestained Protein Ladder (Thermo Scientific).

3.2.6 RDM1-His protein overexpression and purification

pET28a-RDM1 recombinant plasmid was transformed into *E. coli* expression strain Rosetta^{TM}. For RDM1-His protein production one random bacterial colony was inspected. Bacteria were grown on selective LB plates containing Kan and Chl. From overnight bacterial suspensions, cultures for protein induction were made containing the same antibiotics and incubated at 37 °C and 300 rpm until its optical density reached at least 0.6. Protein expression was induced with 1 mM IPTG. After 3 h incubation at 37 °C at 150 rpm, whole proteins were extracted and visualized by SDS-PAGE, CBB staining (**Figure 10A**) and immunodetection (**Figure 10B**). RDM1 fusion protein showed a very strong expression rate. For purification purposes 200 ml of bacterial suspension was used. The same procedure as described above was followed. Bacterial suspensions were centrifuged and washed with 50 mM Tris-HCl pH 8. Bacterial pellet was resuspended in 20 ml His buffer and lysed on ice with 9 ten-second sonication bursts. The lysate was clarified by centrifugation and filtration and 200 µl Ni-NTA resin, previously equilibrated in His lysis buffer, was added. The suspension was incubated overnight at 4 °C and was washed in a series of buffers (W1-W3). Protein elutions from the first purification step were subjected to a second purification

as described in section 2.2.2.3.1.1 to reduce amounts of unspecificaly bound proteins. RDM1-His fusion protein was detected by SDS-PAGE and CBB staining (**Figure 15**). Elutions in **Figure 15A**, showed impure fusion protein due to unspecific binding to Ni-NTA resin, but in large quantities. After the second purification, much of the RDM1-His was lost but the purity was very high (**Figure 15B**). RDM1-His showed a slight shift in electrophoretic mobility in comparison to its theoretical Mw of 22.4 kDa. In total, RDM1-His was expressed and purified in sufficient quantities and outstanding purity to enter pull-down assay.

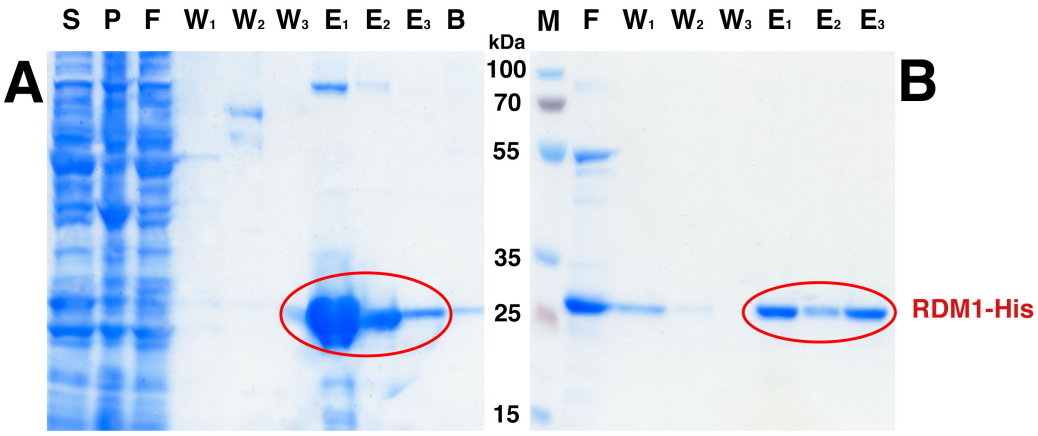

Figure 15. RDM1-His protein detection after SDS-PAGE and CBB staining (circled in red). Theoretical molecular weight for RDM1-His is 22.4 kDa, and here it is detected at 26 kDa. Samples from left to right: supernatant (S), pellet (P), flow through (F), washes (W_1-W_3), elutions (E_1-E_3), resuspended beads (B) after the first **(A)** and second **(B)** affinity chromatography. Extensive washing resulted in protein loss but significant purity. M is Page Ruler^{TM} Plus Prestained Protein Ladder (Thermo Scientific).

3.2.7 WRI1-His protein overexpression and purification

pPROEx-WRI1 recombinant plasmid was transformed into *E. coli* expression strain Rosetta^{TM}. For WRI1-His protein production one random bacterial colony was inspected. Bacteria were grown on selective LB plates containing Amp and Chl. From overnight bacterial suspensions, cultures for protein induction were made containing the same antibiotics and incubated at 37 °C and 300 rpm until its optical density reached at least 0.6. Protein expression was induced with 1 mM IPTG. After 3 h incubation at 37 °C at 150 rpm,

whole proteins were extracted and visualized by SDS-PAGE, CBB staining (**Figure 10A**), and immunodetection (**Figure 10B**). While WRI1-His showed a very elevated expression rate, purified WRI1-His failed to be obtained due to protein aggregation and inclusion body formation (**Figure 16**). Hence, various protocols for soluble protein production were tested. Bacteria were induced with 1 mM IPTG and incubated at 37 °C or 30 °C for 3 h and at 20 °C for 16 h, all at 120-150 rpm. Bacteria were also incubated at 37 °C for 1:30 h or 16 h, and at 20 °C for 1:30 h or 16 h, all at 120-150. IPTG was reduced to 0.4 mM. Further, different lysis buffers were prepared with varying pH (7, 7.6 or 8), increasing Tris-HCl pH 8 and Tris-HCl pH 7.6 to 150 mM and the addition of 10% glycerol. A different buffer system was tried out with 50 mM K_2HPO_4/KH_2PO_4 pH 8 and 0.5 M KCl. Additionally, extraction buffer (20 mM Tris-HCl pH 8, 0.5 M NaCl, 0.1% Triton X-100) as described in Zhai et al. (2017) was used. Cells were disrupted by sonication or lysozyme. The inclusion bodies were always detected in pellet (P) (**Figure 16**). WRI1-His (in pellet) showed a drastic shift in SDS-PAGE mobility compared to its theoretical value of 52.7 kDa.

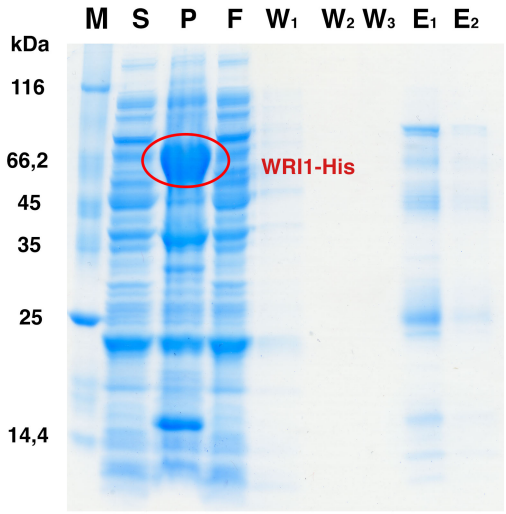

Figure 16. WRI1-His protein detection after SDS-PAGE and CBB staining (circled in red). Theoretical molecular weight for WRI1-His is 52.7 kDa, and here it is detected at 70 kDa. Samples from left to right: supernatant (S), pellet (P), flow through (F), washes (W_1-W_3), elutions (E_1 and E_2). The protein aggregated and was only found in pellet. M is Unstained Protein Molecular Weight Marker (Thermo Scientific™ Pierce™).

3.3 PROTEIN PREPARATION FOR PULL-DOWN ASSAY

After His-tagged protein purification, elution buffer was replaced with 1× PBS to get rid of high imidazole concentration and to prepare proteins for pull-down assay. Because the proteins were purified one by one, some samples stayed for longer periods of time (2-3 weeks) at 4 °C. To test the presence, amount and purity of proteins, and to determinate amount of required protein for pull-down assay, SDS-PAGE, CBB staining (**Figure 17A**) and immunodetection were performed (**Figure 17B**). Although shown to be partially lost during the purification process, this analysis showed that enough protein remained to proceed in pull-down experiment. Abnormal electrophoretic migration of RDM1-His was not observed here.

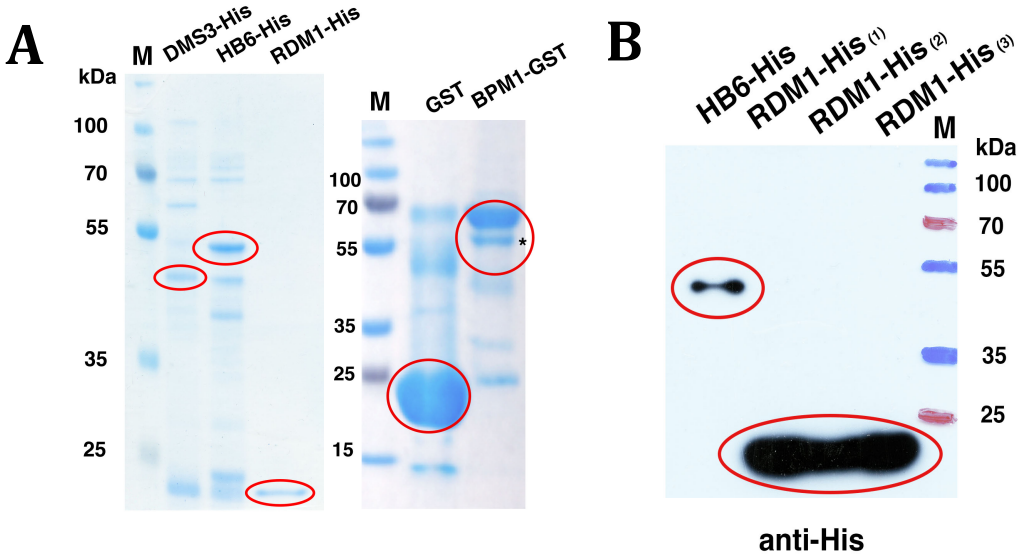

Figure 17. (A) DMS3-His, HB6-His, RDM1-His (first gel) and BPM1-GST and GST as a reference (second gel) (circled in red) after SDS-PAGE and CBB staining. From the intensity of the circled bands, reaction volume of each sample apart from BPM1-GST was calculated. Isoform of BPM1 is noted with an asterisk. **(B)** HB6-His and RDM1-His (circled in red) after immunodetection. Theoretical molecular weight for DMS3-His is 49 kDa, for HB6-His 38.4 kDa, for RDM1-His 22.4 kDa, for BPM1-GST 71 kDa and for GST 26 kDa. M is Page Ruler^{TM} Plus Prestained Protein Ladder (Thermo Scientific).

3.4 PULL-DOWN ASSAY

To test *in vitro* interactions of BPM1-GST protein (bait) attached to glutathione sepharose and His-tagged proteins (prey) one to one, or one to two, reactions were prepared as listed in **Table 4**.

Table 4. Overview of pull-down reactions and negative controls (glutathione S-transferase, GST or glutathione sepharose, GSH) of bait (BPM1-GST) and prey (DMS3-His, HB6-His, RDM1-His) proteins.

PREY(S)	BAIT		
	BPM1-GST	GST	GSH
HB6-His, RDM1-His	+	+	+
HB6-His, DMS3-His	+	+	+
RDM1-His	+	+	+
DMS3-His, RDM1-His	+	+	

3.4.1 BPM1-RDM1 interaction

The interaction between BPM1 and RDM1 was evaluated in one to one pull-down assay. The first experiment was done with 15 µl BPM1-GST attached to glutathione sepharose (bait) and 20 µl of purified RDM1-His (prey). Final volume was adjusted to 1 ml with 1× PBS. For evaluation of effective RDM1-His binding, GST alone attached to glutathione sepharose and glutathione sepharose only (GSH) were used as negative controls. After overnight incubation supernatant was removed, beads washed three times with 1 ml 1× PBS and proteins bound to beads analyzed by anti-His antibody (**Figure 18A**, lanes 6 and 7) and CBB staining (**Figure 18B**, lanes 6 and 7). While CBB-stained membrane revealed BPM1-GST band, no RDM1-His signal was observed (**Figure 18A**, lane 7) probably due to RDM1-His degradation. The whole experiment was therefore repeated with freshly purified RDM1-His. In the second experiment 30 µl BPM1-GST attached to glutathione sepharose (bait) was used. For evaluation of effective RDM1-His binding, GST alone attached to glutathione sepharose and glutathione sepharose only (GSH) were used as negative controls. Purified RDM1-His protein (100 µl) was added to bait and both negative controls and final volume was adjusted to 500 µl with 1× PBS. After overnight incubation supernatant was removed, beads washed three times with 1 ml 1× PBS and proteins bound to beads analyzed by anti-

His antibody (**Figure 19A**, lanes 1-4) and CBB staining (**Figure 19B**, lanes 1-4). There was no interaction of RDM1-His and GST, but RDM1-His interacted equally with glutathione sepharose (GSH) and bait (BPM1).

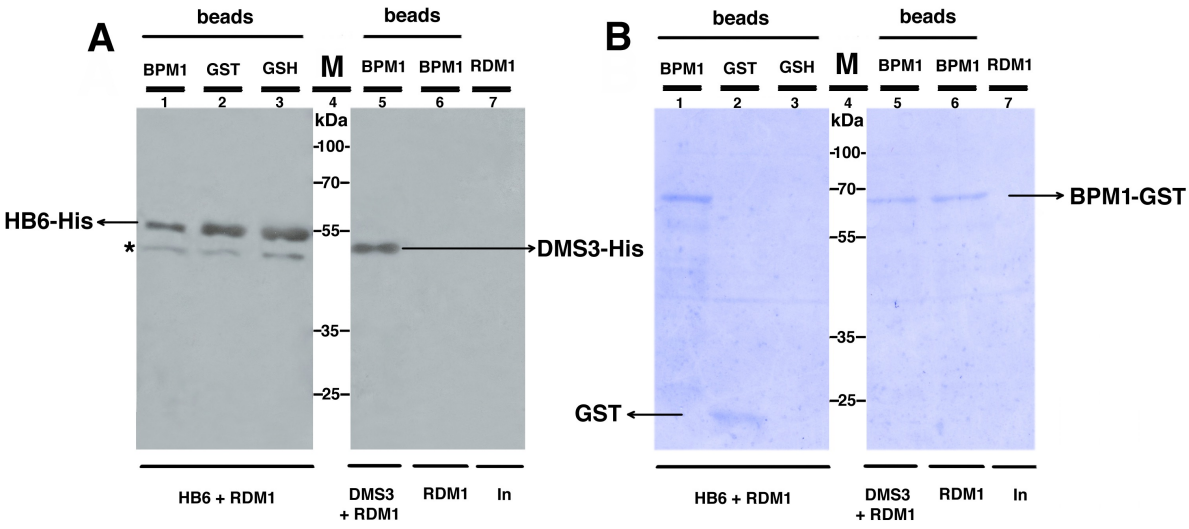

Figure 18. Interaction of BPM1-GST with RDM1-His, HB6-His and DMS3-His proteins after immunodetection with anti-His antibody **(A)** and CBB staining of PVDF membrane **(B)**. BPM1-GST bound to glutathione sepharose was incubated with RDM1-His and HB6-His (lane 1), RDM1-His and DMS3-His (lane 5) or RDM1-His alone (lane 6). Glutathione sepharose (GSH) bound HB6-His with similar intensity as GST attached to glutathione sepharose (lane 2, 3). BPM1-GST attached to glutathione sepharose bound HB6-His to a lesser extent (lane 1). The asterisk indicates a HB6 isoform. No RDM1-His signal was observed probably due to RDM1-His degradation. DMS3-His interacted with BPM1-GST protein (lane 5). RDM1 is 1/10 of input added to reaction (lane 7). M is Page Ruler^{TM} Plus Prestained Protein Ladder (Thermo Scientific).

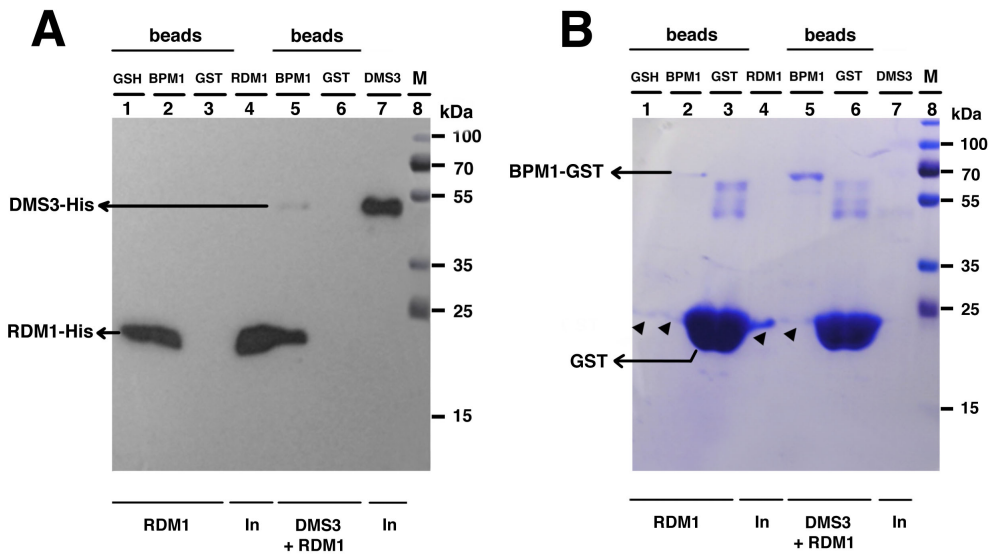

Figure 19. Interaction of BPM1-GST with RDM1-His and DMS3-His proteins after immunodetection with anti-His antibody **(A)** and CBB staining of PVDF membrane **(B)**. BPM1-GST bound to glutathione sepharose was incubated with RDM1-His alone (lane 2) or RDM1-His and DMS3-His (lane 5). Arrowheads point to RDM1-His. Glutathione sepharose (GSH) bound RDM1-His (lane 1) with the similar intensity as BPM1-GST attached to glutathione sepharose (lane 2). RDM1-His did not interact with GST alone attached to glutathione sepharose (lane 3). DMS3-His and RDM1-His interacted with BPM1-GST (lane 5) but not with GST alone (lane 6). RDM1 and DMS3 are 1/10 and 1/3 of input added to reaction (lanes 4 and 7 respectively). M is Page Ruler^{TM} Plus Prestained Protein Ladder (Thermo Scientific).

3.4.2 BPM1 interaction with RDM1 and DMS3

The interaction between BPM1 with RDM1 and DMS3 was evaluated in one to two pull-down assay. In the first experiment, 15 µl BPM1-GST, 15 µl DMS3-His and 20 µl RDM1-His were taken and final volume was adjusted to 1 ml with 1× PBS. For evaluation of effective RDM1-His and DMS3-His binding, GST alone attached to glutathione sepharose and glutathione sepharose only (GSH) were used as negative controls. After overnight incubation supernatant was removed, beads washed three times with 1 ml 1× PBS and proteins bound to beads analyzed by anti-His antibody (**Figure 18A**, lane 5) and CBB staining (**Figure 18B**, lane 5). No RDM1-His signal was detected. DMS3-His interacted equally with BPM1-GST and GST alone, but more intensively with gluthatione beads (GSH). In the second experiment, 30 µl BPM1-GST attached to glutathione sepharose (bait)

was used. For evaluation of effective RDM1-His and DMS3-His binding, GST alone attached to glutathione sepharose was used as negative control. Purified RDM1-His (100 µl) and DMS3-His (30 µl) proteins were added to bait and negative control, and final volume was adjusted to 500 µl with 1× PBS. After overnight incubation supernatant was removed, beads washed three times with 1 ml 1× PBS and proteins bound to beads analyzed by anti-His antibody (**Figure 19A**, lanes 5-7) and CBB staining (**Figure 19B**, lanes 5-7). RDM1-His and DMS3-His interacted with BPM1-GST while there was no interaction of RDM1-His and DMS3-His with GST alone.

3.4.3 BPM1 interaction with RDM1 and HB6

The interaction between BPM1 with RDM1 and HB6 was evaluated in one to two pull-down assay by using 15 µl BPM1-GST attached to glutathione sepharose (bait). For evaluation of effective RDM1-His or HB6-His binding, GST alone attached to glutathione sepharose and glutathione sepharose only (GSH) were used as negative controls. Purified RDM1-His (20 µl) and HB6-His (8 µl) proteins were added to bait and both negative controls and final volume was adjusted to 1 ml with 1× PBS. After overnight incubation supernatant was removed, beads washed three times with 1 ml 1× PBS and proteins bound to beads analyzed by anti-His antibody (**Figure 18A**, lanes 1-3) and CBB staining (**Figure 18B**, lanes 1-3). CBB-stained membrane revealed presence of BPM1-GST but no signal for RDM1-His was observed. HB6-His interacted equally with GST alone and GSH but less intensively to bait (BPM1-GST).

3.4.4 BPM1 interaction with DMS3 and HB6

The interaction between BPM1 with DMS3 and HB6 was evaluated in one to two pull-down assay by using 15 µl BPM1-GST attached to glutathione sepharose (bait). For evaluation of effective DMS3-His or HB6-His binding, GST alone attached to glutathione sepharose and glutathione sepharose only (GSH) were used as negative controls. Purified DMS3-His (15 µl) and HB6-His (8 µl) proteins were added to bait and both negative controls and final volume was adjusted to 1 ml with 1× PBS. After overnight incubation supernatant was removed, beads washed three times with 1 ml 1× PBS and proteins bound to beads analyzed

by anti-His antibody (**Figure 20,** lanes 2-6) and CBB staining (data not shown). DMS3-His interacted equally with GST and bait (BPM1-GST) but considerably more with GSH. HB6-His was only found to interact with GSH. HB6-His was not detected in positive control indicating insufficient addition of HB6-His. On the CBB-stained membrane no BPM1-GST was detected most likely due to bacterial contamination (data not shown).

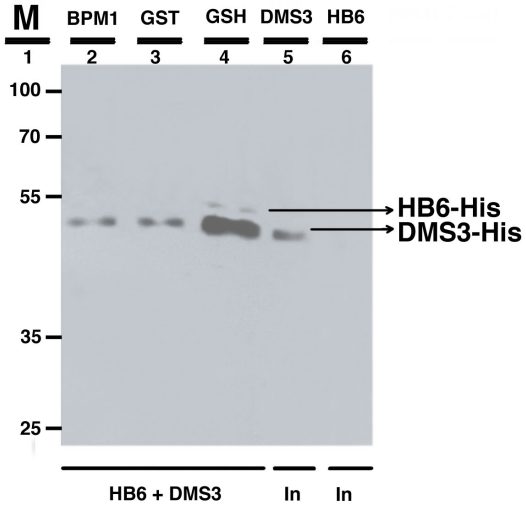

Figure 20. Interaction of BPM1-GST with DMS3-His and HB6-His proteins after immunodetection with anti-His antibody. BPM1-GST bound to glutathione sepharose was incubated with DMS3-His and HB6-His. GST attached to glutathione sepharose bound DMS3-His (lane 3) with similar intensity as BPM1-GST attached to glutathione sepharose (lane 2) but considerably more with glutathione sepharose (GSH) (lane 4). HB6-His was only detected in interaction with GSH. DMS3 and HB6 are 1/10 of input added to reaction (lanes 5 and 6 respectively). No positive control for HB6-His was detected indicating insufficient addition of HB6-His. M is Page Ruler^{TM} Plus Prestained Protein Ladder (Thermo Scientific).

4 DISCUSSION

The aim of this thesis was to purify recombinant BPM1-GST, DMS3-GST, DMS3-His, DREB2A-His, HB6-His, RDM1-His, and WRI1-His *Arabidopsis thaliana* proteins to perform pull-down interaction assays. For this purpose DNA coding sequences of *DMS3, DREB2A, HB6*, *RDM1* and *WRI1* genes were cloned into expression vectors. *DREB2A, HB6* and *WRI1* were successfully cloned into pPROEx expression vector, *RDM1* into pET28a vector and *DMS3* into pGEX4T1 vector. In addition to plasmid constructs generated in this work, plasmid constructs pGEX4T1-BPM1 and pET28a-DMS3 were used for protein overexpression. Recombinant proteins were overexpressed in *E. coli* and purified with established and optimized protocols. Recombinant BPM1-GST, DMS3-GST, DMS3-His, HB6-His and RDM1-His were successfully overexpressed and purified from *E. coli*, while few expression and purification protocols were unsuccessfully employed for DREB2A-His and WRI1-His.

4.1 Protein expression and purification

4.1.1 Inclusion body formation of WRI1

While expressing proteins in a heterologous system like *E. coli*, three main difficulties could arise: low or no expression rate, inclusion body formation and improper processing or posttranslational modification (Duong-Ly and Gabelli, 2014; Rosano and Ceccarelli, 2014).

The second aspect came to the fore when expressing WRI1-His which formed insoluble inclusion bodies found in pellet despite all purification attempts. Protein solubility has been shown to improve by using common strategies such as inclusion of weak promoters, expression at lower temperatures, modified growth media, coexpression with molecular chaperons and fusion with solubility enhancing tags (Smialowski et al., 2007). Here, expression at lower temperatures, lower IPTG concentration, various reaction volumes, with different extraction buffers (presence of glycerol, salt concentration variation, different pH), lysis methods and different incubation times (all featuring changes in growth conditions) were tested without success. Since other proteins did not show the same problem, for the purposes of this research, host strain and vector were not altered.

As reviewed in Idicula-Thomas and Balaji (2005), several works have demonstrated that predicting solubility of a given protein by its primary sequence and its theoretical parameters alone is difficult and of questionable accuracy. Protein solubility is manifested through several sequence-dependent and sequence-independent factors. Inclusion body formation is hence not only influenced by the nature of the protein and its folding process in a sequence-dependent manner but also by the host cell (different pH, osmolarity, redox potential, cofactors, and folding mechanisms), the growth and induction conditions and the level of expression resulting from the vector choice (Duong-Ly and Gabelli, 2014). Overall, high fraction of serine and negatively charged amino acids, higher α-helix propensity and/or less β-sheet propensity are all features associated with improved solubility in *E. coli* (Smialowski et al., 2007). WRI1-His has an overall percentage of 10.7% serines, and 15% overall negatively charged residues. Considering the values, WRI1-His should have been very soluble. Though hydrophobicity is usually correlated with inclusion body formation, the results of this work suggest that it does not have to be the case. Looking at the theoretical aliphatic indexes (AI) (acquired in ProtParam) of all proteins analyzed in this work, WRI1-His exhibits one of the lowest (**Table 2**). The AI is the relative volume occupied by aliphatic side chains of alanine, valine, isoleucine and leucine that can serve as a measure of thermostability of proteins. Therefore, the WRI1-His inclusion body formation cannot be attributed to either the lack of polar and/or negatively charged amino acids or to hydrophobic intermolecular interactions.

Further, it has been reported that improper disulfide bond formation in the reducing environment of the *E. coli* cytoplasm may also contribute to incorrect folding and formation of inclusion bodies. After cell lysis, the proteins are exposed to an oxidizing environment which can promote formation of incorrect disulfide bonds. Consequently, even if disulfide bonds are properly formed in the host, nonnative disulfide bonds between free cysteine residues within and between proteins can form after cell lysis (Duong-Ly and Gabelli, 2014). Given the supplementation of the lysis buffer with reducing agent β-mercaptoethanol, this is a less likely scenario and it does not explain the fact that all other desired proteins were successfully expressed and isolated from the same strain as WRI1-His. Some proteins might be misfolded in a recombinant system because of differences in chaperones or improper interactions with them or other proteins participating in folding. Even

posttranslational modifications such as glycosylation can improve proteins solubility (Duong-Ly and Gabelli, 2014). Both possibilities are highly unlikely, taking into account the successful expression and purification of WRI1-His fusion protein described by Zhai et al. (2017) in *E. coli* BL21 (DE3) strain. Though a very similar protocol was tried out here, WRI1-His was again found to aggregate. Apart from misfolding, proteins might aggregate simply due to high concentration in the solution. Therefore, the incubation time was halved and IPTG concentration reduced, but no difference in solubility was observed.

Taking all these potential causes into account, it is very difficult to pinpoint the exact one for inclusion body formation of WRI1-His. Based on results of Zhai et al. (2017) there is strong indication that the cause of inclusion body formation might be connected to very specific induction and/or purification conditions used here. To overcome this problem, WRI1 could be expressed as a fusion protein carrying a tag that increases solubility like maltose binding protein (MBP) or thioredoxin (Trx; Smialowski et al., 2007). Alternatively, bacteria could be cotransformed with chaperones in combination with alternations in incubation conditions. It would also be possible to purify proteins from pellet and refold them, but the refolding process is often very laborious and challenging (Smialowski et al., 2007).

4.1.2 Low overexpression of DREB2A

Low or no expression of a heterologous protein in *E. coli* may be due to differences from the source organism in compartmentalization and environment, chaperones, codon usage bias, protein instability, inefficient translation and cell toxicity (Duong-Ly and Gabelli, 2014). Since prior to expression the construct was properly cloned and sequenced, and its existence proved in bacteria, low expression is more likely to be attributed to downstream factors.
Before addressing the individual possibilities listed above in context to inefficient DREB2A-His production it should be noted that there might be more than one cause and that one cannot rule out the other. Firstly, codon usage bias observed in prokaryotic translation of eukaryotic genes can be excluded as a potential cause for no expression because Rosetta™ strain used here contains pRARE plasmid which carries genes for tRNAs rarely used in prokaryotes (Rosano and Ceccarelli, 2014). Secondly, inefficient translation could arise if

DNA sequence of a gene contains inverted repeats that form stem-loops in mRNA which hinder the activity of ribosomes. By submitting the *DREB2A* CDS sequence to RNAfold WebServer (http://rna.tbi.univie.ac.at/cgi-bin/RNAWebSuite /RNAfold.cgi), many complementary sequences in its mRNA were detected. Therefore, hindrance to protein translation could at least to some extent affect low expression rate of this protein.

Protein instability is another possible cause. *In planta*, overexpressed DREB2A-His was shown to be destabilized through a PEST sequence (Sakuma et al., 2006) and was therefore very hard to detect in normal growth conditions (Qin et al., 2008; Morimoto et al., 2017). However, in heterologous systems, especially in bacteria that do not recognize PEST sequences, this feature is not relevant. In the analysis of theoretical instability index (II; measure for predicting protein stability in a test tube) calculated in ProtParam (**Table 2**), DREB2A-His was marked as an unstable protein. The same applied to HB6-His which was observed to be lost in considerable amounts after protein extraction and in every other purification step, likely due to protease degradation during protein extraction, protein degradation in buffer afterwards and/or protein precipitation. Unexpectedly, RDM1-His was marked as unstable too, but showed to be stable over longer periods of time. Furthermore, the presence of certain amino acids in the first position after fMet, namely arginine, lysine, phenylalanine, leucine, tryptophan or tyrosine, is correlated with short half-life in bacteria (Duong-Ly and Gabelli, 2014). None of them were found on N-terminus of DREB2A, implying no correlation to its instability and low expression rates.

DREB2A-His might require unique chaperones and/or posttranslational modifications for stability. The opposite was proved when Morimoto et al. (2017) showed successful DREB2A-His production in *E. coli* where it was expressed as a Trx-6× His fusion protein, containing apart from histidine, a thioredoxin tag. It is possible that DREB2A is somehow stabilized by it. Sometimes, protein degradation may occur after cell lysis when proteases come into contact with overexpressed proteins. However, given the conditions under which the experiment was carried out (keeping samples on ice, using protease inhibitors in lysis buffer and expressing proteins in strains deficient in some proteases) it is most unlikely to be a relevant possibility here.

Cell toxicity is one further possibility. Some proteins, e.g. membrane proteins, proteins that interact with DNA or interfere with electron transport can have a negative effect on cell

growth. After multiple attempts at induction of DREB2A-His expression in *E. coli*, it has been shown that cells carrying pPROEx-DREB2A construct exhibit retarded growth compared to cells transformed with other constructs. Additionally, these cells formed very small colonies on agar selective plates, compared to all other transformants. It could be that "leaky" basal expression prior to protein induction occurs and that this has a negative effect on cell growth. In this context it is worth mentioning that Morimoto et al. (2017) used a Rosetta^{TM} [DE3] pLys strain for DREB2A protein expression in which leaky expression is completely prevented. As the name suggests, it contains a plasmid, pLys, which, among other, encodes a T7 lysozyme that inhibits T7 RNA polymerase and therefore protein transcription in uninduced conditions. DE3 strains are T7 lysogens, containing λDE3 prophage inserted in the chromosome of the bacteria that encodes a T7 RNA polymerase. These strains are often used when the gene of interest is placed under the strong T7 promoter. The basal expression of T7 polymerase and therefore the desired protein, can be controlled by lysozyme coexpression which inhibits polymerase activity (Rosano and Ceccarelli, 2014). pPROEx vector, however, to which *DREB2A* was cloned, does not contain such a T7 promoter. Cotransformation with pLys would therefore not have an effect on protein expression. But the fact that the authors used such a specific strain supports the possibility of leaky expression and protein toxicity to be the cause of low protein production of DREB2A-His in *E. coli*.

Taken together, these results indicate that low and no expression of DREB2A-His most likely occurred due to protein instability or host toxicity. The main molecular mechanism for either of two possibilities in which they affect protein expression in *E. coli* remains unclear. Keeping this in mind, however, different strategies to overcome the problem can be developed. Cell toxicity, for instance, could be overcome by directing protein secretion to periplasm or media using an N-terminal signal. Other options include lowering incubation temperature, induction at higher OD_{600} value and addition of glucose into medium. Alternatively, a less sensitive *E. coli* strain or a different vector could be selected (Duong-Ly and Gabelli, 2014). For overcoming instability, coexpression with chaperones could be tested (Duong-Ly and Gabelli, 2014).

As an endnote to this topic of protein overexpression in *E. coli*, theoretical AI and II have proven to be (in some cases) inconsistent with the observed results. This makes the analysis, as noted on the ProtParam online website itself, only a potential guidance for handling protein samples. Moreover, they are to be determined experimentally for each protein like protein solubility.

4.2 Macromolecule electrophoretic mobility

In denaturing SDS polyacrylamide gel electrophoresis in general, proteins migrate according to their molecular weight in presence of SDS molecules (Pitt-Rivers and Impiombato, 1968). On one hand, it is due to binding an equal amount of negatively charged SDS per weight, which "swamps out" the intrinsic charge of the protein. On the other, it is the disruption of protein shapes in presence of SDS molecules (Mattice et al., 1976). Here, however, SDS-PAGE analysis for most induced fusion proteins revealed a slight to drastic shift in electrophoretic mobility. Even if stable homodimers formed in the purification process, no observed protein weight corresponded to the sum of individual theoretical masses of proteins. Since prokaryotes do not possess a very broad spectrum of covalent posttranslational modification systems like ubiquitylation, there are limited possibilities of it being the cause of drastic shifts in protein mobility. Only phosphorylation could be connected to slighter SDS-PAGE migration abnormality. Fusion tags might be partially responsible for this anomaly as well.

The apparent molecular mass for e.g. HB6-His showed to have a mass of 52 kDa (**Figure 14**) instead of the expected 38.4 kDa. Similar anomaly is also observed in Lechner et al. (2011) and Himmelbach et al. (2002). Also, in Lechner et al. (2011) HB6 was shown to have two isoforms as detected here (**Figures 14** and **18**). WRI1-His band showed mobility of approximately 70 kDa (**Figure 16**), significantly higher than its predicted molecular mass of 52.7 kDa. In Zhai et al. (2017) electrophoretic mobility differ from expected and is shown to be 70 kDa, like here. After analyzing the amino acid sequence of both (HB6-His and WRI1-His) proteins, the anomalous behavior in SDS-PAGE could be attributed to a high content of negative residues (Graceffa et al., 1992; Alves et al., 2004). HB6-His has 18%, while WRI1-His contains 15% negatively charged amino acids (aspartate and glutamate) with relatively low amounts of positively charged amino acids such as arginine or lysine. As pointed out in

Graceffa et al. (1992), the negative charge of aspartate and glutamate could repulse negative SDS molecules. Consequently, the protein might bind less of SDS, leading to insufficient denaturation and, accordingly, to slow migration in gel. The exact explanation for the influence of negatively charged residues in reducing the electrophoretic mobility of proteins remains, however, unclear (Graceffa et al., 1992).

BPM1-GST showed a slighter shift in comparison to HB6-His and WRI1-His (**Figures 11** and **17**) with an observed mass of around 60 kDa in comparison to its theoretical value of 71 kDa. Given that GST showed a similar shift on gel as well, the BPM1-GSTs abnormal behavior could be the consequence of GSTs modification or structural change. BPM1-GST and GST alone showed an increased SDS-PAGE mobility, unlike HB6-His and WRI1-His. Negative charged residues are speculated, as mentioned above, to repulse SDS molecules. Following the same logic, increased mobility in electrophoresis may be due to attraction of positively charged amino acids for SDS. On the other hand, it has been shown that disulfide bond formation in oxidizing environment can also increase mobility (Dunker and Kenyon, 1976). Looking at the sequences of both BPM1-GST and GST, neither the former nor the latter seem to have a great relative abundance of positively charged residues. As for the other possibility, the sample buffer, which was added to proteins prior to loading onto gel contained β-mercaptoethanol that reduced disulfide bonds. Two other possibilities include generation of truncated proteins by premature dissociation of RNA polymerase from DNA template generating shortened mRNAs or due to premature translation termination. Finally, it should be noted that such a shift in gel electrophoresis of BPM1 and GST was not detected in previous works and that their abnormal mobility might be attributed to specific experimental conditions carried out here, e.g. different polyacrylamide gel or buffers used.

RDM1-His showed at first an abnormal electrophoretic behavior migrating as a 26 kDa protein (**Figure 15**) but normalized afterwards when it migrated equal to its theoretical Mw of 22.4 kDa (**Figure 17**). A possible explanation for the observed slow migration could be attributed to macromolecule asymmetry rich in secondary helical structure (Graceffa et al., 1992; Alves et al., 2004), with RDM1 showing a similar one (Allard et al., 2005). Insufficient denaturation of proteins with many postulated strong salt bridges in such a structure, causes increase in frictional resistance in PAGE (Graceffa et al., 1992). Nevertheless, since RDM1-His mobility normalized after buffer replacement, it is more

likely that either pH or the composition of buffer itself or different polyacrylamide gel used for electrophoresis might have had an effect on its mobility. It is possible that both structure and conditions had an effect on SDS-PAGE mobility here.

Proteins are not the only macromolecules that show different mobility rates in an electric field in electrophoretic methods. Small variations in DNA agarose gel electrophoretic mobility has also been proven (Stellwagen and Stellwagen, 2009). The cause lies in different DNA conformations: the linear, circular supercoiled or circular relaxed DNA. Plasmids are present in circular and mostly negatively supercoiled form inside bacteria. After digestion, DNA becomes linearized and runs faster in gels than the relaxed one, but slower than the supercoiled DNA (Stellwagen and Stellwagen, 2009). Supercoiled DNA molecules have a more compact conformation than linear DNAs containing the same number of base pairs, and migrate much faster than linear DNA molecules. Relaxed DNAs have negligible mobility in electrophoresis, presumably because they are impaled by dangling fibers in the matrix (Stellwagen and Stellwagen, 2009). Here, no notable difference was observed in digestion verification of final constructs but small differences could be detected after the restriction of initial constructs (data not shown). After DNA purification from agarose gels, the ligation or In-Fusion solutions contained most likely partially undigested relaxed plasmid DNA. They were found in considerably lower amounts than the digested one, leading to no considerable difficulties in the cloning process.

4.3 Pull-down interaction assay

Pull-down assay is an *in vitro* technique for studying direct protein interactions of purified proteins. This assay is sometimes a better choice for protein interaction studies in terms of limited participants and defined environment than e.g. yeast two hybrid (Y2H) assays where false positive results can easily arise (Ito et al., 2001). What should be taken into account, however, is the protein production in a heterologous system (*E. coli*). Proteins require a precise three-dimensional conformation for their activity and interactions. The establishment of proper protein conformation include processes like protein folding in general (formation of secondary and tertiary structure), spontaneous or enzyme catalyzed *cis*-isomerization of

prolines, disulfide bond formation, posttranslational covalent modifications (e.g. glycosylation) and proteolysis (Alberts et al., 2008; Nelson and Cox, 2008). In a heterologous system like *E. coli* these processes might to some extent differ. Therefore adequate negative controls should be taken into account to avoid false positive results. At the same time negative results do not have to necessarily indicate the lack of interaction that might occur in *in vivo* conditions. It is also worth mentioning that pull-down assay, while a valuable technique for studying stable interactions, transient protein-protein interactions are almost impossible to detect because the complex may dissociate during the assay.

In this experiment, taking into account all papers published on pull-down assays between BPM1 and its interactors (Weber and Hellmann, 2009; Lechner et al., 2011; Chen et al., 2013, 2015), several possible outcomes were anticipated. If BPM1 showed a considerable higher affinity for either of the two proteins (HB6 or RDM1/DMS3) in the mixture, only one would bind to it, forcing out the other. If, however, BPM1 bound both proteins with similar affinity, the binding rate would be divided between two interactors. Since HB6 and DMS3 are both speculated to bind to MATH domain of BPM1 (Lechner et al., 2011), their binding might be of competitive nature. Preliminary research has shown that the binding of RDM1 related with the BTB domain of BPM1. HB6 and RDM1 might therefore simultaneously bind to BPM1.

Here, pull-down assay between BPM1 and RDM1 was carried out for the first time. Equal interactions between BPM1-GST and RDM1-His, and glutathione sepharose (GSH) and RDM1-His were observed (**Figure 19**). A possible cause for signal absence of RDM1-His in the first experiment (**Figure 18**) could have been protein degradation during storage and incubation period. In the second pull-down experiment, both DMS3-His and RDM1-His were observed to interact with BPM1-GST but not with glutathione S-transferase (GST) alone (**Figure 19**). While DMS3 was shown in previous research to directly interact with BPM1 but not with GST alone (Bauer et al., 2014), RDM1 and DMS3 were demonstrated to interact *in vitro* and *in vivo* (Law et al., 2010). Based on these results it could be presumed that RDM1 might interact with BPM1 via DMS3. The opposite was demonstrated when the above mentioned one to one pull-down assay between RDM1 and BPM1 was conducted.

Previous, unpublished results show interaction of DMS3-His and BPM1-GST in pull-down assay but not with GST alone. The same was demonstrated with BPM1-GST and *in vitro* expressed HB6 (Lechner et al., 2011). In contrast to these results, in the one to two pull-down assays between BPM1, HB6 and DMS3 or RDM1, interactions of both HB6-His and DMS3-His with GST and additionally, GSH, were observed (**Figures 18** and **20**). Because none of the published papers used the additional negative control of GSH, no comparisons with existing data could be made. Glutathione sepharose might have a strong affinity for proteins as DMS3-His and HB6-His were found to bind it more tightly than BPM1-GST and/or GST alone. Compared to the reaction incubation periods (1-2 h) in the above mentioned works, the different interaction profile observed here could be a consequence of long incubation time (at least 16 h), different binding buffer used and/or different input volumes of proteins taken.

The one to two pull-down assay between BPM1, HB6 and DMS3 showed DMS3-His to be the only interaction partner of BPM1-GST (**Figure 20**). As mentioned above, DMS3-His also interacted with both GST and GSH. HB6-His was shown to bind GSH while protein amounts in other samples were beyond the sensitivity of immunodetection. This interaction pattern could potentially indicate competitive binding between the two prey proteins where DMS3-His forced out HB6-His in the binding process. Since signals in negative controls for both proteins were detected, no definite conclusion could be made and the assay should be repeated. A third one to two pull-down assay between BPM1, HB6 and RDM1 was performed. Since HB6-His showed interactions with both GST and GSH (negative controls), and RDM1-His being degraded, the test was not informative about their interaction. Pull-down assay should therefore be repeated.

Throughout the course of the experiment and pull-down assay conduct, a general issue of low protein concentration arose. It was best demonstrated when a one to one and one to two pull-down assay for BPM1, RDM1 and DMS3 was repeated, where the total volume was cut by a half and protein input volumes increased. The immunodetection of this second assay showed much more promising results. Also, the age and storage conditions of protein solutions could have a vital influence on the outcome of an experiment. In this case it was the likely degradation of RDM1 during storage at 4 °C. Future experiments should therefore

be executed with larger protein concentrations and in lower reaction volumes. Protein samples with which pull-down assay is to be performed should also be freshly prepared.

Had the proteins been eluted with free glutathione, discernment between GSH-bound and BPM1-GST or GST-bound proteins could have been made. However, protein binding to GST alone still presents a difficulty for interaction analysis in a pull-down assay. Normally, the interaction between GST and prey proteins is a strong indicator that pull-down assay is not a suitable test for interaction studies of desired proteins. In the second, repeated pull-down experiment between RDM1, DMS3 and BPM1, however, proteins did not interact with GST alone. This suggests that some conditions in which the first pull-down assays were performed were likely the cause of their interactions with GST. To avoid false positive results detected here, binding buffer and incubation time could be modified. Also, resin where the reactions were carried out could be replaced with, e.g. magnetic beads. Replacing fusion tags by cloning the genes into different vectors is also a valid mean to overcome this problem. Alternatively, had all reactions been a one to one protein interaction study, BPM1-GST could have been pulled-down by His-tagged proteins. The proteins would be bound to Ni-NTA resin the same way GST-tagged proteins were bound to glutathione sepharose. In that context, it would be possible, as described in Lapetina and Gil-Henn (2017), to determine the dissociation constant, K_d, for each described protein to BPM1. The K_d is an equilibrium constant that specifies the tendency of a complex to reversibly dissociate into initial compounds. That would allow the comparison of binding affinities of different proteins to a given binding partner. K_d can also be determined with alternative methods as mentioned and described in more detail in Pollard (2010). Regardless, binding reactions vary in strength. Hence, the answer to whether two molecules interact with each other should always be quantitative with a number that describes the affinity (Pollard, 2010).
BPM1 (Weber et al., 2005), DMS3 (Kanno et al., 2008), RDM1 (Allard et al., 2005) and HB6 (Harris et al., 2011) have all shown to form homodimers *in vitro* and/or *in vivo.* Homodimer formation should be taken into consideration when investigating protein interactions. It is possible that homodimers are more steadily formed than heterodimers or that the sequences for hetero- and homodimerization even overlap and interfere. Additionally, pull-down reactions with proteins containing reverse tags could also be

conducted. In this case, BPM1 combined with histidine and its interaction partners with GST. That way it would be possible to determine whether tags somehow interfere with the interactions in question.

The overall obtained results of pull-down assays imply that conditions in which the reactions were carried out were unfavorable for protein interaction studies between BPM1, HB6 and RDM1 or DMS3. Consequently, modified pull-down and other protein interaction assays are needed to investigate interaction of selected proteins. In general, *in vitro* assays are limited systems for studying molecular mechanisms since they do not entirely reflect *in vivo* circumstances (though binding buffer is physiologic in both pH and ionic strength). Hence, it would be favorable if both *in vitro* and *in vivo* assays could be carried out for testing protein interactions.

5 CONCLUSION

To conclude, DNA coding sequences of five *Arabidopsis thaliana* genes were successfully cloned into expression vectors. *DREB2A, HB6* and *WRI1* were cloned into pPROEx expression vector, *RDM1* into pET28a vector and *DMS3* into pGEX4T1 vector. Recombinant BPM1-GST, DMS3-GST, DMS3-His, HB6-His and RDM1-His were successfully overexpressed and purified from *Escherichia coli* with established protocols. Despite several attempts, no protocol was optimized for overexpression of DREB2A-His or purification of WRI1-His. To compare the binding affinity of BPM1 to its potential interactors, pull-down reactions between the fusion protein BPM1-GST and its protein partners HB6-His, DMS3-His and RDM1-His were carried out. Under reaction conditions described here, BPM1 was shown to interact with RDM1 and DMS3. In a pull-down assay between RDM1, HB6 and BPM1, no RDM1 signal was observed, while HB6 was bound to BPM1 and GST alike. In a pull-down assay between DMS3, HB6 and BPM1, DMS3 interacted with both BPM1 and GST, while HB6 did not interact with either of them. RDM1, HB6 and DMS3 were all found to bind to glutathione sepharose (GSH).

6 REFERENCES

Ahmad K. F., Engel C. K. and Prive G. G. (1998): Crystal structure of the BTB domain from PLZF. Proceedings of the National Academy of Sciences of the USA **95:** 12123–12128.

Alberts B., Johnson A., Lewis J., Raff M., Roberts K. and Walter P. (2008): Molecular Biology of the Cell. Garland Science, New York.

Allard S. T. M., Bingman C. A., Johnson K. A., Wesenberg G. E., Bitto E., Jeon W. B. and Phillips G. N. (2005): Structure at 1.6 A resolution of the protein from gene locus At3g22680 from *Arabidopsis thaliana*. Acta Crystallography, Section F **61**: 647-650.

Alves V. S., Pimenta D. C., Sattlegger E. and Castilho B. A. (2004): Biophysical characterization of Gir2, a highly acidic protein of *Saccharomyces cerevisiae* with anomalous electrophoretic behavior. Biochemical and Biophysical Research Communications **314:** 229-234.

Bauer N., Leljak-Levanić D., Vuković R. and Razdorov G. (2014): MATH-BTB domain protein AtBPM1 directly interact with DMS3, important component of RNA-directed DNA methylation in plants. FEBS-EMBO Paris, France, 30.8.-4.9.2014, pp. 306-306.

Chen L., Bernhardt A., Lee J. H. and Hellmann H. (2015): Identification of *Arabidopsis* MYB56 as a Novel Substrate for $CRL3^{BPM}$ E3 Ligases. Molecular Plant **8**: 242–250.

Chen L., Hyun Lee J., Weber H., Tohge T., Witt S., Roje S., Fernie A. and Hellmann H. (2013): *Arabidopsis* BPM proteins function as substrate adaptors to a CULLIN3-based E3 ligase to affect fatty acid metabolism in plants. The Plant Cell **25:** 2253–2264.

Dunker A. K. and Kenyon A. J. (1976): Mobility of sodium dodecyl sulphate - protein complexes. Biochemistry Journal **153**: 191–197.

Duong-Ly K. C. and Gabelli S. B. (2014): Explanatory Chapter: troubleshooting recombinant protein expression: general. Methods in Enzymology **541**: 209-229.

Focks N. and Benning C. (1998): Wrinkled1: a novel, low-seed-oil mutant of *Arabidopsis* with a deficiency in the seed-specific regulation of carbohydrate metabolism. Plant Physiology **118**: 91–101.

Gao Z. H., Liu H. L., Daxinger L., Pontes O., He X., Qian W., Lin H., Xie M., Lorković Z. J., Zhang S., Miki D., Zhan X., Pontier D., Lagrange T., Jin H., Matzke A. J., Matzke M., Pikaard C. S. and Zhu J. K. (2010): An RNA polymerase II- and AGO4-associated protein acts in RNA-directed DNA methylation. Nature **465:** 106–109.

Gingerich D. J., Gagne J. M., Salter D. W., Hellmann H., Estelle M., Ma L. and Vierstra R. D. (2005): Cullins 3a and 3b assemble with members of the broad complex / tram- track / bric-a-brac (BTB) protein family to form essential ubiquitin–protein ligases (E3s) in *Arabidopsis*. The Journal of Biological Chemistry **280:** 18810–18821.

Gingerich D. J., Hanada K., Shiu S. H. and Vierstra R. D. (2007): Large-scale, lineage-specific expansion of a bric- a-brac / tramtrack / broad complex ubiquitin-ligase gene family in rice. Plant Cell **19:** 2329–2348.

Graceffa P., Jancsó A. and Mabuchi K. (1992): Modification of acidic residues normalizes sodium dodecyl sulfate-polyacrylamide gel electrophoresis of caldesmon and other proteins that migrate anomalously. Archives of Biochemistry and Biophysics **297:** 46-51.

Grimberg A., Carlsson A. S., Marttila S., Bhalerao R. and Hofvander P. (2015): Transcriptional transitions in *Nicotiana benthamiana* leaves upon induction of oil synthesis by WRINKLED1 homologs from diverse species and tissues. BMC Plant Biology **15**: 192-208.

Haag J. R. and Pikaard C. S. (2011): Multisubunit RNA polymerases IV and V: Purveyors of non-coding RNA for plant gene silencing. Nature Reviews, Molecular Cell Biology **12**: 483–492.

Harris J. C., Hrmova M., Lopato S. and Langridge P. (2011): Modulation of plant growth by HD-Zip class I and II transcription factors in response to environmental stimuli. The New Phytologyst **190:** 823–837.

Himmelbach A., Hoffmann T., Leube M., Hohener B. and Grill E. (2002): Homeodomain protein ATHB6 is a target of the protein phosphatase ABI1 and regulates hormone responses in *Arabidopsis*. The EMBO Journal **21**: 3029–3038.

Idicula-Thomas S. and Balaji P. V. (2005): Understanding the relationship between the primary structure of proteins and its propensity to be soluble on overexpression in *Escherichia coli.* Protein Science **14**: 582–592.

Ito T., Chiba T., Ozawa R., Yoshida M., Hattori M. and Sakaki Y. (2001): A comprehensive two-hybrid analysis to explore the yeast protein interactome. Proceedings of the National Academy of Sciences of the USA **98(8):** 4569-4574.

Kanno T., Bucher E., Daxinger L., Huettel B., Bohmdorfer G., Gregor W., Kreil D. P., Matzke M. and Matzke A. J. (2008): A structural- maintenance-of-chromosomes hinge domain-containing protein is required for RNA-directed DNA methylation. Nature Genetics **40:** 670–675.

Koegl M., Hoppe T., Schlenker S., Ulrich H. D., Mayer T. U. and Jentsch S. (1999): A novel ubiquitination factor, E4, is involved in multiubiquitin chain assembly. Cell **96:** 635-644.

Lapetina S. and Gil-Henn H. (2017): A guide to simple, direct, and quantitative *in vitro* binding assays. Journal of Biological Methods **4(1):** e62.

Larkin M. A., Blackshields G., Brown N. P., Chenna R., McGettigan P. A., McWilliam H., Valentin F., Wallace I. M., Wilm A., Lopez R., Thompson J. D., Gibson T. J. and Higgins D. G. (2007): Clustal W and Clustal X version 2.0. Bioinformatics **23(21):** 2947-2948.

Law J. A., Ausin I., Johnson L. M., Vashisht A. A., Zhu J. K., Wohlschlegel J. A. and Jacobsen S. E. (2010): A protein complex required for polymerase V transcripts and RNA-directed DNA methylation in *Arabidopsis*. Current Biology **20**: 951–956.

Lechner E., Leonhardt N., Eisler H., Parmentier Y., Alioua M., Jacquet H., Leung J. and Genschik P. (2011): MATH/BTB CRL3 Receptors Target the Homeodomain-Leucine Zipper ATHB6 to Modulate Abscisic Acid Signaling. Developmental Cell **21:** 1116–1128.

Leljak-Levanić D., Horvat T., Martinčić J. and Bauer N. (2012): A novel bipartite nuclear localization signal guides BPM1 protein to nucleolus suggesting its Cullin3 independent function. PLoS ONE **7(12):** e51184.

Lorković Z. J., Naumann U., Matzke A. J. and Matzke M. (2012): Involvement of a GHKL ATPase in RNA-Directed DNA Methylation in *Arabidopsis thaliana.* Current Biology **22**: 933–938.

Ma W., Kong Q., Mantyla J. J., Yang Y., Ohlrogge B. J. and Benning C. (2016): 14-3-3 protein mediates plant seed oil biosynthesis through interaction with AtWRI1. The Plant Journal **88**: 228–235.

Maeo K., Tokuda T., Ayame A., Mitsui N., Kawai T., Tsukagoshi H. and Ishiguro S. K. (2009): An AP2-type transcription factor, WRINKLED1, of *Arabidopsis thaliana* binds to the AW-box sequence conserved among proximal upstream regions of genes involved in fatty acid synthesis. The Plant Journal **60**: 476–487.

Mattice W. L., Riser J. M. and Clark D. S. (1976): Conformational properties of the complexes formed by proteins and sodium dodecyl sulfate. Biochemistry **15:** 4264-4272.

Matzke M. A. and Mosher R. A. (2014): RNA-directed DNA methylation: an epigenetic pathway of increasing complexity. Nature Reviews Genetics **15(6):** 394-408.

Maupin-Furlow J. (2011): Proteasomes and protein conjugation across domains of life. Nature Reviews Microbiology **10(2):** 100-111.

Mazzucotelli E., Belloni S., Marone D., De Leonardis A. M., Guerra D., Di Fonzo N., Cattivelli L. and Mastrangelo A. M. (2006): The E3 ubiquitin ligase gene family in plants: regulation by degradation. Current Genomics **7(8):** 509–522.

Morimoto K., Ohama N., Kidokoro S., Mizoi J., Takahashi F., Todaka D., Mogami J., Sato H., Qin F., Kim J. S., Fukao Y., Fujiwara M., Shinozaki K. and Yamaguchi-Shinozaki K. (2017): BPM-CUL3 E3 ligase modulates thermotolerance by facilitating negative regulatory domain-mediated degradation of DREB2A in *Arabidopsis.* Proceedings of the National Academy of Sciences of the USA **114(40):** 8528-8536.

Nelson D. L. and Cox M. M. (2008): Lehninger principles of biochemistry. W.H. Freeman, New York.

Pintard L., Willis J. H., Willems A., Johnson J. L., Srayko M., Kurz T., Glaser S., Mains P. E., Tyers M., Bowerman B. and Peter M. (2003): The BTB protein MEL-26 is a substrate-specific adaptor of the CUL-3 ubiquitin-ligase. Nature **425**: 311-316.

Pitt-Rivers R. and Impiombato F. S. A. (1968): The binding of sodium dodecyl sulphate to various proteins. Biochemical Journal **109**: 825-830.

Pollard T. D. (2010): A Guide to Simple and Informative Binding Assays. Molecular Biology of the Cell **21(23):** 4061-4067.

Qin F., Sakuma Y., Tran L. S., Maruyama K., Kidokoro S., Fujita Y., Fujita M., Umezawa T., Sawano Y., Miyazono K., Tanokura M., Shinozaki K. and Yamaguchi-Shinozaki K. (2008): Arabidopsis DREB2A-interacting proteins function as RING E3 ligases and negatively regulate plant drought stress-responsive gene expression. Plant Cell **20:** 1693–1707.

Ream T. S., Haag J. R., Wierzbicki A. T., Nicora C. D., Norbeck A. D., Zhu J. K., Hagen G., Guilfoyle T. J., Pasa-Tolic L. and Pikaard C. S. (2009): Subunit compositions of the RNA-silencing enzymes Pol IV and Pol V reveal their origins as specialized forms of RNA polymerase II. Molecular Cell **33**: 192–203.

Rosano G. L. and Ceccarelli E. A. (2014): Recombinant protein expression in *Escherichia coli*: advances and challenges. Frontiers in Microbiology **5:** 172-188.

Sakuma Y., Maruyama K., Qin F., Yuriko Y., Shinozaki K. and Yamaguchi-Shinozaki K. (2006): Dual function of an *Arabidopsis* transcription factor DREB2A in water-stress-responsive and heat-stress-responsive gene expression. Proceedings of the National Academy of Sciences of the USA **103(49):** 18822-18827.

Smialowski P., Martin-Galiano A. J., Mikolajka A., Girschick T., Holak T. A. and Frishman D. (2007): Protein solubility: sequence based prediction and experimental verification. Bioinformatics **23(19):** 2536-2542.

Stellwagen N. C. and Stellwagen E. (2009): Effect of the matrix on DNA electrophoretic mobility. Journal of Chromatography A **1216(10):** 1917–1929.

Sunnerhagen M., Pursglove S. and Fladvad M. (2002): The new MATH: homology suggests shared binding surfaces in meprin tetramers and TRAF trimers. FEBS Letters **530:** 1–3.

Vainonen J. P., Jaspers P., Wrzaczek M., Lamminmaki A., Reddy R. A., Vaahtera L., Brosche M. and Kangasjarvi J. (2012): RCD1-DREB2A interaction in leaf senescence and stress responses in *Arabidopsis thaliana*. The Biochemical Journal **442:** 573–581.

van den Heuvel S. (2004): Protein Degradation: CUL-3 and BTB - Dispatch Partners in Proteolysis. Current Biology **14**: 59–61.

Weber H. and Hellmann H. (2009): *Arabidopsis thaliana* BTB⁄ POZ-MATH proteins interact with members of the ERF⁄AP2 transcription factor family. FEBS Journal **276**: 6624–6635.

Weber H., Bernhardt A., Dieterle M., Hano P., Mutlu A., Estelle M., Genschik P. and Hellmann H. (2005): *Arabidopsis* AtCUL3a and AtCUL3b form complexes with members of the BTB ⁄ POZ-MATH protein family. Plant Physiology **137**: 83–93.

Wierzbicki A. T., Cocklin R., Mayampurath A., Lister R., Rowley M. J., Gregory B. D., Ecker J. R., Tang H. and Pikaard C. S. (2012): Spatial and functional relationships among Pol V-associated loci, Pol IV-dependent siRNAs, and cytosine methylation in the *Arabidopsis* epigenome. Genes and Development **26:** 1825–1836.

Yamaguchi-Shinozaki K. and Shinozaki K. (2006): Transcriptional regulatory networks in cellular responses and tolerance to dehydration and cold stresses. Annual Reviews Plant Biology **57**: 781–803.

Zemach A., Kim M. Y., Hsieh P. H., Coleman-Derr D., Eshed-Williams L., Harmer S. L. and Zilberman D. (2013): The *Arabidopsis* nucleosome remodeler DDM1 allows DNA methyltransferases to access H1-containing heterochromatin. Cell **153:** 193–205.

Zhai Z., Liu H. and Shanklin J. (2017): Phosphorylation of WRINKLED1 by KIN10 Results in its Proteasomal Degradation, Providing a Link Between Energy Homeostasis and Lipid Biosynthesis. Plant Cell **29(4):** 871-889.

Zhang H., Ma Z. Y., Zeng L., Tanaka K., Zhang C. J., Ma J., Bai G., Wang P., Zhang S. W., Liu Z. W., Cai T., Tang K., Liu R., Shi X. and Zhu J. K. (2013): DTF1 is a core component of RNA-directed DNA methylation and may assist in the recruitment of Pol IV. Proceedings of the National Academy of Sciences of the USA **110:** 8290–8295.

Zheng B., Wang Z., Li S., Yu B., Liu J. Y. and Chen X. (2009): Intergenic transcription by RNA polymerase II coordinates Pol IV and Pol V in siRNA-directed transcriptional gene silencing in *Arabidopsis*. Genes and Development **23(24):** 2850-2860.

http://rna.tbi.univie.ac.at/cgi-bin/RNAWebSuite/RNAfold.cgi (accessed 15 January 2019)

http://rsb.info.nih.gov/ij/download.html (accessed 16 September 2018)

http://www.merckmillipore.com/INTL/en/product/RosettaDE3-Competent-CellsNovagen,EMD_BIO-70954 (accessed 10 November 2018)

https://web.expasy.org/protparam/ (accessed 5 Dezember 2018)

https://web.expasy.org/translate (accessed 5 Dezember 2018)

https://www.addgene.org/vector-database/ (accessed 19 February 2018)

https://www.arabidopsis.org/ (accessed 19 February 2018)

https://www.ncbi.nlm.nih.gov/ (accessed 19 February 2018)

https://www.neb.com/products/c2987-neb-5-alpha-competent-e-coli-high-efficiency# Product Information (accessed 10 November 2018)

https://www.takarabio.com/learning-centers/cloning/in-fusion-cloning-tools (accessed 1 March 2018)

https://www.takarabio.com/products/cloning/competent-cells/stellar-chemically-competent-cells (accessed 10 November 2018)

https://www.thermofisher.com/ (accessed 20 January 2019)

CURRICULUM VITAE

Personal information

Name: Mirta Tokić

Education

2016 – 2019 Graduate program of Molecular Biology, University of Zagreb, Faculty of Science, Department of Biology
2013 – 2016 Undergraduate program of Molecular Biology, University of Zagreb, Faculty of Science, Department of Biology

Training

Laboratory practice in the Plant Molecular Biology Laboratory, University of Zagreb, Faculty of Science, Department of Biology
Lab Demonstrator for the course Genetic Engineering in Biotechnology

Skills

Languages: Croatian (mother tongue), German (proficient) and English

Digital competence: Microsoft Office

Hobbies: painting and drawing, sports, hiking